

## **General Disclaimer**

### **One or more of the Following Statements may affect this Document**

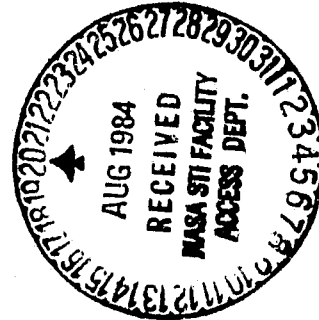
- This document has been reproduced from the best copy furnished by the organizational source. It is being released in the interest of making available as much information as possible.
- This document may contain data, which exceeds the sheet parameters. It was furnished in this condition by the organizational source and is the best copy available.
- This document may contain tone-on-tone or color graphs, charts and/or pictures, which have been reproduced in black and white.
- This document is paginated as submitted by the original source.
- Portions of this document are not fully legible due to the historical nature of some of the material. However, it is the best reproduction available from the original submission.

(NASA-TM-77506) STABILIZED LUMINOUS ARCS  
(ROTATING ARCS) IN NITROGEN AND CARBON  
DIOXIDE AT PRESSURES OF ONE TO FORTY  
ATMOSPHERES (National Aeronautics and Space  
Administration) 58 p HC A04/MF A01 CSCL 20C G3/33 20041 N84-29095  
Unclassified

STABILIZED LUMINOUS ARCS (ROTATING ARCS) IN  
NITROGEN AND CARBON DIOXIDE AT PRESSURES OF ONE  
TO FORTY ATMOSPHERES

Rudolf Foitzik

Translation of "Untersuchungen am stabilisierten  
elektrischen Lichtbogen (Waelzbogen) in Stickstoff  
und Kohlensaeure bei Druecken von 1 bis 40 at.",  
Wissenschaftliche Veroffentlichungen aus dem Siemens-  
Werken, Vol. 19, No. 1940, pp. 28-58.



NATIONAL AERONAUTICS AND SPACE ADMINISTRATION  
WASHINGTON D.C. 20546 AUGUST 1984

OPTIONAL FORM E  
OF THE CLOUDY CITY

STANDARD TITLE PAGE

1. Report No. NASA TM-77506	2. Government Accession No.	3. Recipient's Catalog No.	
4. Title and Subtitle STABILIZED LUMINOUS ARCS (ROTATING ARCS) IN NITROGEN AND CARBON DIOXIDE AT PRESSURES OF ONE TO FORTY ATMOSPHERES		5. Report Date August, 1984	6. Performing Organization Code
7. Author(s)  Rudolf Foitzik		8. Performing Organization Report No.	9. Work Unit No.
9. Performing Organization Name and Address  SCITRAN Box 5456 Santa Barbara, CA 93108		10. Contract or Grant No. NASW 3542	11. Type of Report and Period Covered Translation
12. Sponsoring Agency Name and Address  National Aeronautics and Space Administration Washington, D.C. 20546		13. Supplementary Notes Translation of "Untersuchungen am stabilisierten elektrischen Lichtbogen (Waelzbogen) in Stickstoff und Kohlensaeure bei Druecken von 1 bis 40 at.", Wissenschaftliche Veröffentlichungen aus dem Siemens-Werken, Vol. 19, No. 1940, pp. 28-58.	
14. Abstract The arcs were run in the axis of a rapidly rotating glass tube, at 1-20 atm. For pressures over 20 atm., a decrease of stability appeared and above 40 atm., the results were very unsatisfactory owing to turbulence. The voltage and longitudinal-field-strength curves for both gases had a descending character. The field strength was 1.5-2.0 times as high in CO <sub>2</sub> as in N. Under 10 atm. of pressure approx. linear values obtained. In N the column diam. increased with pressure. C. d. increased with pressure in CO <sub>2</sub> . Good agreement with the Steenbeck "Minimum principle" was in general obtained.			
15. Key Words (Selected by Author(s))		16. Distribution Statement  Unclassified and Unlimited	
17. Security Classif. (of this report) Unclassified	18. Security Classif. (of this page) Unclassified	19. No. of Pages 58	20. Price

STABILIZED LUMINOUS ARCS (ROTATING ARCS) IN NITROGEN AND  
CARBON DIOXIDE AT PRESSURES OF ONE TO FORTY ATMOSPHERES

/28\*

By Rudolf Foitzik, Neubabelsberg High Voltage Institute of the  
Berlin Institute of Technology and Switch Plant of the  
Siemens-Schuckert Works, Inc., at Siemensstadt

(Submitted on September 8, 1939)

C O N T E N T S

	PAGE
I. Introduction	4
II. Procedure	6
III. Measurement device testing	9
a) Effect of the stabilizing tube's rate of rotation on the column's stabilization	10
b) Effect of the stabilizing tube's temperature on arc voltage	12
c) Effect of the glass tube's optical distortion on the photographically determined arc diameter	15
IV. Measurement results	15
1. Measurements in nitrogen	15
a) Current voltage characteristics at different pres- sures	15
b) Determination of the longitudinal field intensity from current voltage characteristics	18
c) Column diameter measurement by current density determination	21
d) Dependence of current density on current intensity, pressure and longitudinal field intensity	24
2. Measurements in carbon dioxide	29
a) Current voltage characteristics and longitudinal	30

\* Numbers in the right margin indicate the foreign pagination

	PAGE
field intensity	
b) Column diameter and current density	32
V. Comparison between measurement results and theory	34
a) Arc column conductivity in nitrogen	34
b) Arc column energy in nitrogen	40
c) Current and pressure dependence of the longitudinal field intensity according to the minimum principle	44
d) Column diameter and column temperature pressure depend- ence according to the minimum principle	49
VI Conclusion	53

SUMMARY In order to obtain reproducible measurement results, the arc burns on the axis of a rapidly rotating glass tube (rotating arc). It is supplied with direct current of between 1 and 20 A. In nitrogen an increasing loss of stability can be observed above 20 atm. Above 40 atm it was no longer possible to obtain a stable arc, due to turbulence. At the larger stabilization tube diameter (5 cm diameter as compared to 3 cm diameter) and also in the presence of carbon dioxide, the stabilization conditions became unfavorable already at 10 atm, as the pressure was increased.

The measurements show that the current-voltage and the current-longitudinal field intensity curves are of a decreasing nature, for nitrogen and carbon dioxide, also at high pressures. Numerically, the values of the longitudinal field intensity are higher for carbon dioxide (approximately 1 1/2 to 2 times higher) than for nitrogen, at the same current and pressure. In nitrogen the longitudinal field intensity is nearly constant at low current

intensities (, J A), as a function of pressures up to 10 atm. Up to 5 atm there is even a slight decrease, with increasing pressure. At both current intensities above 6 A and also at pressures above 10 atm, the field intensity increases between 1 and 10 atm at a linear rate, even at low current intensities and thus differs from the behavior with nitrogen.

In nitrogen, the arc diameter increases with increasing pressure, i.e., the current density decreases at increasing pressure, in contrast to carbon dioxide, where the current density increases with increasing pressure.

The measurement results are related to the known theoretical expressions for current transport, ionization and energy, as well as an extreme condition: Steenbeck's Minimum Theory of Arc Voltage.

For nitrogen, we found that the course of the longitudinal field intensity calculated according to the theory of the smallest burning voltage, as well as the current density are in good agreement with the measurement results, as a function of current intensity and pressure. In addition, the results from the minimum theory - that at constant column diameter the temperature is nearly independent of pressure and increases with increasing column diameter - are also in good agreement with the results obtained from the measurements.

/58

\*

A series of publications are already available on the electric arc under increased pressure. L. Duncan, A. J. Rowland and R. J. Todd [1]\* have studied the arc at pressures up to 10 atm, O. Lummer [2] to 25 atm, G. P. Luckey [3] to 35, W. Mathiesen [4] to 6 atm.

While the test of the first of these authors were intended to verify the then existing theory of the electric arc, subsequent studies had a special technical purpose: O. Lummer tried to obtain the highest possible temperatures, by increasing the pressure, as well as increasing the light yield. It was also W. Mathiesen's goal to obtain increased intensity and economy for the electric arc at increased pressure, for illumination purposes, while it was G. P. Luckey's goal to melt tungsten for the fabrication of light bulbs.

Even though these tests were partially successful, they did not contribute much knowledge regarding the actual behavior of the arc, i.e., regarding the dependence of physical data on arc discharges on pressure.

/29

The reason for this is that the electric arcs investigated in the publications mentioned did not burn under conditions satisfactory to unobjectionable measurements. They were short arcs, throughout, in which mutual interference occurred between the various segments of the discharge.

It was only the application of an effective stabilization method [5.6] that made it possible to produce and study long electric arc discharges under defined, clean conditions, as shown by W. Grotrian's [7] first measurements and others, as

---

\* Numbers in square brackets indicate the References listed at the end of this publication

those by A. von Engel [8,9,10]. The main result of W. Grotrian's tests was that the carrier gas is of decisive importance for the electric arc and that the nature of the electrodes is secondary, in comparison. Since the column of stabilized arcs represents the most significant portion of the discharge, the interest in experimental and theoretical studies on this matter moved to the foreground.

In addition to the experiments with the electric arc stabilized by air turbulence, arcs of high current intensity at extremely high current densities in the column were also subjected to intensive investigation [12-15, 18]. However, to date no information has been published on experiments regarding the pressure dependence of the individual process variables of the stabilized column, above 1 atm.

While as yet there is no strict theory to describe the details of arc discharges under a variety of conditions, the theoretical postulates regarding the basic physical processes in the arc discharge lead to equations that fairly adequately reproduce the arc's variable measured under careful test conditions. In this context the minimum theory has been particularly fruitful, as first applied by M. Steenbeck [16] to the electric arc. It states that under certain prescribed conditions, the electric arc will so adjust its variable magnitudes that its electrode tension will adopt the smallest value possible.

Although no rigorous proof has been supplied yet for the validity of the minimum theory, and its veracity is being questioned [17], according to the work of F. Kesselring [18], R. Holm, B. Kirschstein and F. Koppelman [19,20], it does not contradict their observations. However, because the radial temperature decrease is ignored in the column, only an approximated description of the actual conditions can be expected.

Since the minimum theory represents a still lacking but needed

supplementary condition to the basic equation for the stationary arc discharge, the current carrier equation, and the ionization and energy relationship, it is in principle possible to describe the physical magnitudes in the electric arc column, without using empirical variables.

It must hence be considered of interest to verify the minimum theory's applicability through further observational material. Studies of the pressure dependence of arc columns are especially suited to this purpose.

Therefore it is the purpose of this study to perform the most careful measurements possible on the stabilized column of a direct current discharge, at different currents and pressures, /30 and to relate the results to the current, and especially, the pressure dependence of the variable quantities of the arc column, calculated from the minimum theory.

## II PROCEDURE

For the current intensities of up to approximately 25 A under consideration, two stabilization methods can be considered: air turbulence stabilization according to P. Scheinherr (5-7) and rotating arc stabilization according to R. Holm (9, 10). Air turbulence stabilization is especially suited to the generation of extremely long arcs, but has disadvantages. Based on a logical application of Reynolds' law of similarity\*, air turbulence stabilization must

---

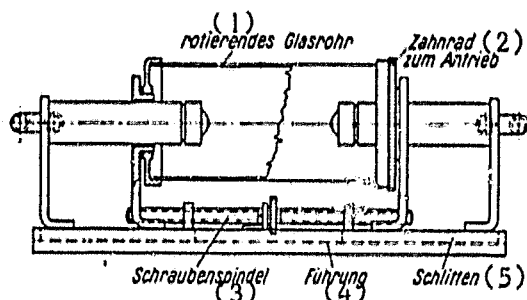
\* According to O. Reynolds, we can expect mechanical similarity between two systems when  $\frac{\rho_1 \cdot w_1 \cdot l_1}{\mu_1} = \frac{\rho_2 \cdot w_2 \cdot l_2}{\mu_2} = \text{const}$ , where  $l_1, l_2$  are characteristic lengths;  $w_1, w_2$  are characteristic flow velocities;  $\mu_1, \mu_2$  are viscosities and  $\rho_1, \rho_2$  are densities. There will be turbulence once the constant exceeds a certain characteristic value (Reynolds number). The viscosity or internal friction of gases is independent of the pressure (except near the vaporization temperature). The density is approximately proportional to the pressure, here. The radius of the air turbulence may be considered the characteristic length.

be expected to decrease considerably, at high pressures, since the tendency to form turbulent vortexes - which is particularly great for air turbulence stabilized arcs - increases proportionally as the pressure does. In contrast, in rotating arcs under otherwise equal conditions (tube diameter, electrode shape, angular velocity of the air turbulence or glass tube, respectively), turbulent vortexes and hence, stabilization disruptions, will occur only at substantially higher pressures.

In addition, while for rotating arcs the stabilizing gas mass performs a purely rotating motion, especially in the arc's midportion, and hence accomplishes a homogeneous release of energy along the arc column, in the case of air turbulence stabilization there is a gas mass translation superimposed over the rotation, in the feed direction. Thereby the energy removal and hence the longitudinal field intensity decreases along the arc column, due to increased gas heating. However, at atmospheric pressure this decrease in longitudinal field intensity appears to be of subordinate importance [9], but at higher pressures the effect is not readily apparent.

In addition to the above considerations, the application of rotating arc stabilization in these studies was favored above all by the fact that the rotating arc is particularly amenable to theoretical energy considerations, because it involves only heat conduction and heat radiation for energy dissipation, and especially heat convection plays no role here, while in principle it can not be neglected in the air turbulence stabilized arc.

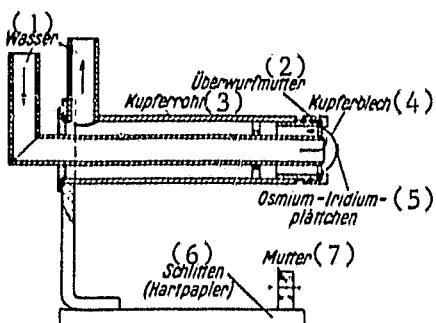
Stabilization by the rotating arc principle occurs through a high-melting point glass tube of either 3 or 5 cm diameter, rotating rapidly around the column axis, impelled by a small electric motor over a cogwheel. The glass tube's rotation rate could be adjusted within wide limits, to a maximum of 3400 rpm. Figure 1 (page 8) shows a section through the device. /31



KEY 1 Rotating glass tube 2 Driving cogwheel 3 Lead screw 4 Guideways 5 Sliding cradle

Figure 1 Rotating arc arrangement

The two arc electrodes consisted of high melting point metals (osmium-iridium tips and tungsten) attached to a thin copper sheet on the frontal side of a water-cooled copper tube. A section of the electrodes can be seen in Figure 2, below. The



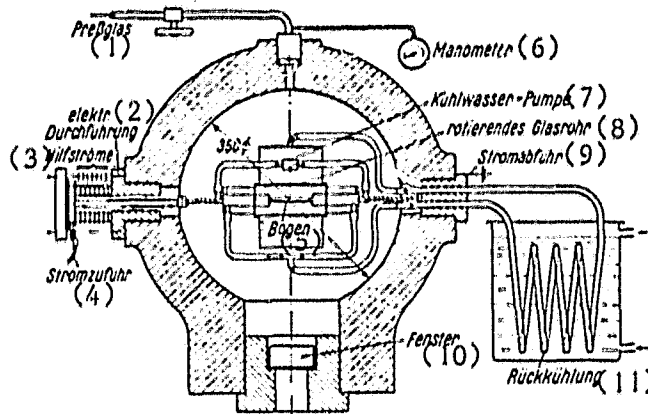
KEY 1 Water 2 Screw cap 3 Copper tube 4 Copper sheet 5 Osmium-iridium tips 6 Carriage (laminated paper) 7 Nut

Figure 2 Arc electrode section

electrodes were arranged in a closed steel container, because of the increased pressure, and were not accessible during the experiment. The distance between the electrodes (arc length) was therefore changed with the aid of an electric motor in the pressurized container. The electrode distance could be read off outside of the container, through a special electric contactor and transmitter; it could be precisely adjusted, to 0.02 cm. The

largest electrode distance was 8.7 cm.

The pressure container had been checked to an excess pressure of 100 atm. Figure 3, below, shows a schematic of the entire



KEY 1 Pressed glass 2 Electrode lead-in 3  
Auxiliary current 4 Power supply 5 Arc 6 Manometer  
7 Cooling water pump 8 Rotating glass tube 9 Ground  
10 Window 11 Recooling

Figure 3 Schematic of the pressure container with multiple electric lead-ins, electric arc apparatus and water cooling circuit

electric arc arrangement. The device for water-cooling the electrodes can be seen, the multiple electric lead-ins for high pressure, to activate ancillary equipment and the window for photographic records of the arc. The arc is supplied by two direct current generators in series, which can take loads of up to 25 A at 1000 V, together. The ohmic resistance of the cooling water, in parallel to the arc, had a value of from 2 to  $3 \cdot 10^5$  Ohm.

### III MEASUREMENT DEVICE TESTING

Before beginning with the actual measurements at the rotating arc, it was considered necessary to identify any sources of error, which can easily be present in electric arc arrangements, to reduce them to a minimum by the appropriate methods, or

ORIGINAL PAGE IS  
OF POOR QUALITY

conversely, to be able to estimate them, should they occur in any event, to take them into account in the discussion of any results.

a) Effect of the stabilization tube's rate of rotation on the column's stabilization

Just as in the air turbulence stabilized arc, in the rotating arc stabilization depends, by its nature, on the rate of rotation of the stabilizing gas masses, and more specifically for the rotating arc, on the rotation rate of the stabilization tube. It is to be expected that in order to obtain effective stabilization, i.e., to obtain an arc that burns evenly and horizontally in the electrode axis, a minimum rotation rate of /32

TABLE I Minimum rotation rate in rotating arc stabilization for various pressures and current intensities. Tube diameter: 3 cm

Druck (3) at	Stickstoff (1)			Druck (3) at	Kohlensäure (2)		
	ungeführter Strom (4) A	Mindestdrehzahl (5) U/min etwa	Strom etwa (6) A		Mindestdrehzahl (5) U/min		
1	2	300	1	1	3		400
1	15	500	1	10			800
5	6	1000	3	3			800
10	8	2000	3	10			1200
20	4	2500	5	2,5			1500
20	15	3000	5	10			2000
30	5	über 3400	8	2,5			2300
40			8	10			2000
			10	3			3000
			10	10			über 3400
			15	4			-

KEY 1 Nitrogen 2 Carbon dioxide 3 Pressure, atm 4 Approximate current, A 5 Minimum rotation rate, rpm approximately 6 Current A, approx.

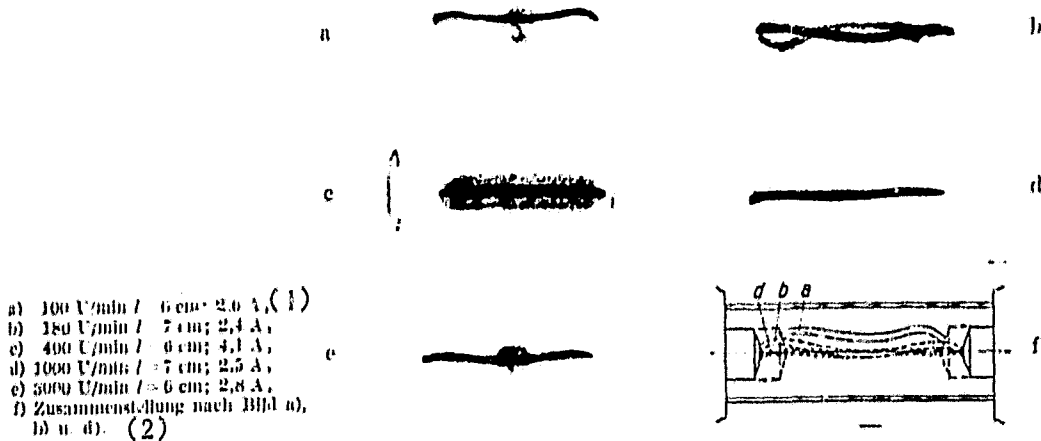
the glass tube was necessary, which in each case depends on the arc's operating data.

In order to be certain of effective stabilization during the electric arc measurements, in each case, this minimum rotation rate was determined for various current intensities and pressures, both by visual observation and through photographic

records of the arc. This information is shown in Table 1, above, for nitrogen and carbon dioxide. It should be remarked that stabilization occurs slowly, at increasing rotation rates and hence that the minimum rotation rate is not sharply defined. The values shown in Table 1, based in every case on several observations, must hence not be considered precise measurement values, but serve merely as indications for the measurements to be performed.

As can be seen in Table 1, the minimum rotation rate increases both with increasing current intensity and increasing pressure, and is higher throughout for carbon dioxide than for nitrogen. At 30 atm, complete stabilization could no longer be attained, at intermediate current intensities and the highest obtainable rotation rate of 3400 rpm. For carbon dioxide, however, under the same conditions stabilization became disturbed already at 10 atm.

Further increases in the rotation rate - which were not possible in the arrangement used, however - presumably would have been unsuccessful, since at these pressures, as we mentioned in section 2, turbulent flow precludes stabilization. One may assume, rather, that at pressures above approximately 40 atm, electric arc stabilization by means of rotating gas masses is no longer possible, with stationary electrodes, since then the minimum rotation rate already lies within ranges in which interfering turbulence occurs. The photographic records in Figure 4 show the start of stabilization at increasing rotation rates. The example shows arcs in carbon dioxide at 1 atm pressure. At low rotation rates (Figure 4a), the arc occurs above the axis (more readily visible in the diagram of Figure 4f) and has a nearly horizontal position only due to the presence of the glass tube. /33 At higher rotation rates the central arc portions are already forced into the arc axis; the edge portions, for which the stabilizing effect is diminished due to the friction of the rotating gases against the non-rotating electrodes, are not yet



KEY 1 U/min = rpm 2 Composite, from 4a, 4b and 4d

Figure 4 Effect of the rotation rate of a 3 cm diameter tube on the stabilization of a rotating arc in carbon dioxide at 1 atm

so forced. The arc is generally quite unstable in this course, and the point of support often rapidly varies its location. At Figure 4c the minimum rotation rate has finally been attained and stabilization is satisfactory. Further increases in the rotation rate are without effect both on stabilization and on the arc voltage.

b) Effect of the stabilizing tube's temperature on arc voltage

If it is assumed that energy is released primarily by heat conduction, then theoretical considerations on the energy balance in the rotating arc indicate that the energy released (and hence the arc voltage) are dependent on the stabilizing tube's temperature. Since it is difficult, in this rotating arc arrangement oriented towards pressure studies to maintain the temperature of the rotating stabilization tube constant through cooling, it became necessary to examine the effect of the tube temperature on the arc voltage, as dependence of the arc voltage on current intensity and arc burn duration. In Table 2 (page 13) are shown the results of such measurements:

ORIGINAL PAGE IS  
OF POOR QUALITY

TABLE 2 Effect of burn duration of a rotating arc at constant current intensity, in nitrogen at 1 atm in a 3 cm diameter tube, on arc voltage

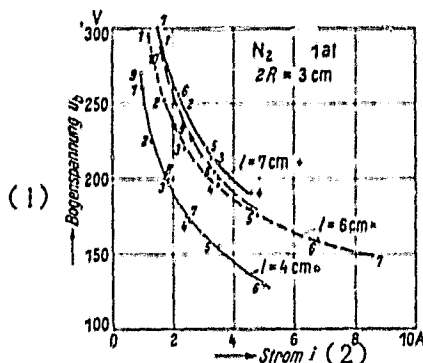
Brenndauer des Bogens sec (1)	(2) Bogenlänge 4 cm		(2) Bogenlänge 7 cm		(2) Bogenlänge 8 cm		(2) Bogenlänge 9 cm	
	Strom (3)	Spannung (4)	Strom (3)	Spannung (4)	Strom (3)	Spannung (4)	Strom (3)	Spannung (4)
0	1,62	214	2,04	268	1,6	332	12,6	126
10	1,62	214	2,03	266	1,6	330	12,3	124
20	1,60	216	2,04	262	1,6	328	12	140
30	1,60	212	2,02	266	1,58	334	—	—
35	—	—	2,0	270	1,57	350	—	—
40	1,61	212	1,98	280	—	550	—	—
45	—	—	1,96	295	—	—	—	—
50	1,6	215	—	—	—	—	—	—

KEY 1 Arc burn duration, sec 2 Arc length 3 Current 4 Voltage

These measurements generally coincide in showing that the arc voltage initially remains constant or decreases slightly, to then increase more or less steeply after a certain time; this /34 increase occurs sooner and is steeper at higher currents and greater arc lengths, than at smaller currents and shorter arc column lengths. At an arc length of 4 cm and at 1.6 A, no substantial change had occurred after 3/4 of a minute.

This behavior by the arc voltage can be explained as follows: the gradual decrease in arc voltage is related to the decreasing energy release through heat conduction. The subsequent rise in arc voltage can presumably be attributed to some interfering effect, conceivably the vaporization of fat layers from the stabilization tube deposits; these tubes become quite hot, and especially for long arcs (8 cm). When the fat vapors enter the arc column, they are degraded to hydrogen, which causes the increase in voltage.

These were orienting experiments for subsequent photographic techniques. The arc was always ignited by contact, at low current intensities, and then rapidly adjusted to the length to be examined. At low currents and pressures, approximately 4 to 5 measurement points were recorded, at large currents and high



KEY 1 Arc voltage 2 Current

Figure 5 Current-voltage characteristics of rotating arcs for increasing and decreasing current intensity, for test purposes

pressures, only 3, 2 or 1 measurement points were recorded. As a control, following the last measurement point the lowest current of the corresponding series was applied again, and the instruments were read\*. If the control point showed a voltage increase at this point, determined by an already excessive burn time for the arc at the corresponding current intensity and pressures, then the measurement series was either not used at all, or only partially.

Figure 5 shows examples of flawless measurement series, for the two arc lengths 4 and 7 cm, with the measurement sequence indicated by the numerical order.

It can be seen that at a pressure of 1 atm and small currents 7-9 measurement points were taken with the 7 cm or respectively, 4 cm long arc, without any noticeable voltage increase occurring. In contrast, the curve for the 6 cm arc length is an example of a useless or only partially usable measurement series, in Figure 5, above (1 atm, 10 measurement points). Here the control measurement points already show significant voltage increases, due to excessive arc burn duration. In such cases it

\* As a rule the current intensity was then slightly lower than initially, because of the heating of the arc's resistance

is possible to observe a weak glowing in the tube, once the arc has been extinguished.

c) Effect of the glass tube's optical distortion on the photographically determined arc diameter

For a precise determination of the diameter of the arc column burning along the axis of the rotating stabilizing tube, it is necessary to know any possible distortion during the recording /35 (photographing) through the glass tube. The calculation from optical refraction laws is not altogether simple. But since this in any event would not take into consideration the special characteristics of the glass tube used - index of refraction, striation, not-rounded areas, etc. - it was preferred to perform an experimental determination of the diameter distortion, on a rotating tube. To this end, a strip of millimeter-graded graph paper was affixed axially between the fixed supports, and photographed. From several photographs so obtained, using different glass tubes, no radial distortion in axial segments could be found.

#### IV MEASUREMENT RESULTS

##### 1. Measurements in nitrogen

###### a) Current-voltage characteristics at different pressures

Figure 6 (page 16) shows a family of curves of current-voltage characteristics for a 6 cm arc length at measured pressures between 1 and 40 atm. The effect of pressure can be readily seen: at constant current intensity the arc voltage increases with increasing pressure. In addition, while at low pressures the arc voltage decreases, up to the highest current intensities measured, at higher pressures it already attains a constant value, or respectively, it approaches the minimum known from other studies [3]. This arc voltage minimum is interpreted as

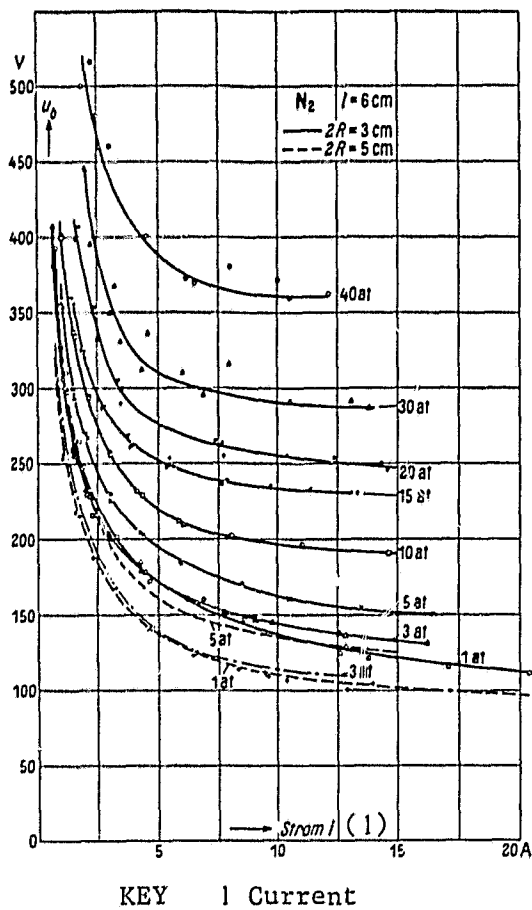
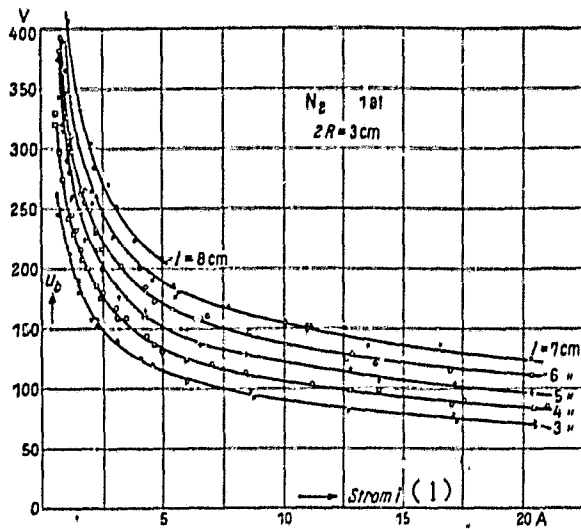


Figure 6 Current-voltage characteristics of rotating arcs of constant length in nitrogen, from 1 to 40 atm

an edge effect, in the stabilized arc.

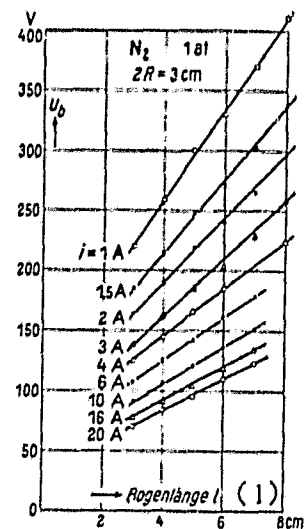
We shall just add that at pressures of up to 20 atm there is little scatter in the measurement points, but that at higher pressures the scatter of the measurement points also increases. In addition to a significant flattening of the arc column, the decrease in or failure of stabilization at high pressures also causes increasing instrument restlessness and hence, increased imprecision in the values read on them. Thus, the measurement values obtained at 40 atm, especially, must already be considered useless for any subsequent investigations. The current-voltage characteristics obtained at other arc lengths produce families

ORIGINAL PAGE IS  
OF POOR QUALITY



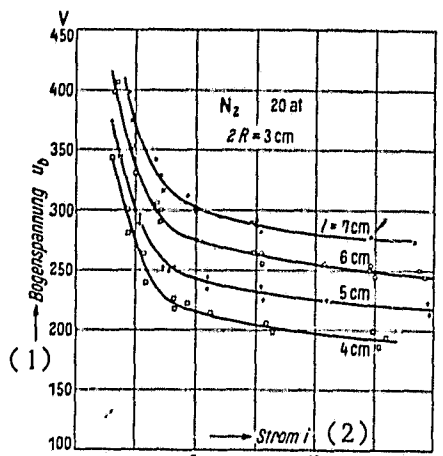
KEY 1 Current

Figure 7 Current-voltage characteristics of a rotating arc, in nitrogen at 1 atm, for various arc lengths



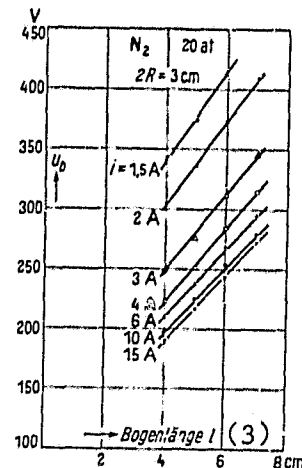
KEY 1 Arc length

Figure 8 Arc voltage dependence on arc length in rotating arcs, in 1 atm of nitrogen



KEY 1 Arc voltage 2 Current

Figure 9 Current voltage characteristics of rotating arcs of various lengths in nitrogen, at 20 atm



KEY 1 Arc length

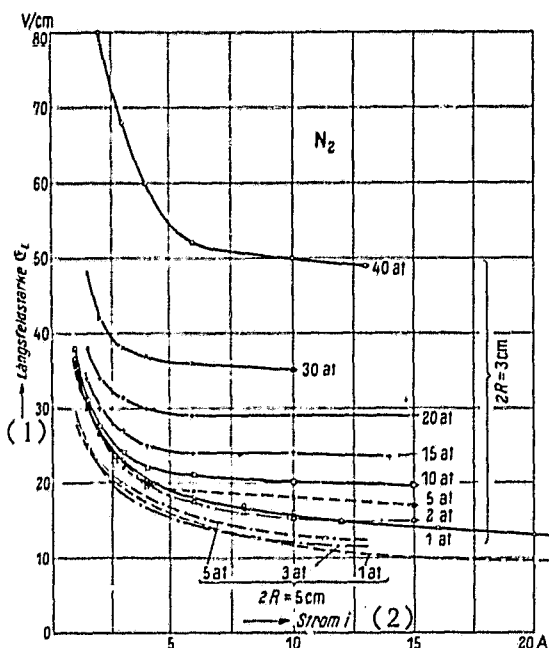
Figure 10 Arc voltage dependence on arc length for various currents, for longitudinal field intensity determination

of curves similar to those of Figure 6. However, we shall not dwell any longer on the details of current-voltage characteristics, since they are not particularly relevant to this study. They are used only in arc column longitudinal field intensity determination.

b) Determination of the longitudinal field intensity from current-voltage characteristics

In order to determine the longitudinal field intensity, families of current-voltage curves were obtained in each case, for different arc lengths, usually between 3 and 8 cm, at 1 cm intervals.

Two such families of curves - for 1 and 20 atm - are shown as an example, in Figures 7 and 9 (page 17). In these families of curves, initially the arc voltages were plotted as a function of arc length, at constant current, in the usual manner. As can be seen in Figures 8 and 10 (page 17), the corresponding points lie on a straight line, with adequate precision; this indicates that the field intensities were constant, in the arc column segment investigated. /37



KEY 1 Longitudinal field intensity 2 Current 3 Carrier gas pressure

Figure 11 Longitudinal field intensity  $G_L$  of rotating arc columns in nitrogen, at 1 to 40 atm and 3 and 5 cm tube diameters, as a function of the current  $i$ .

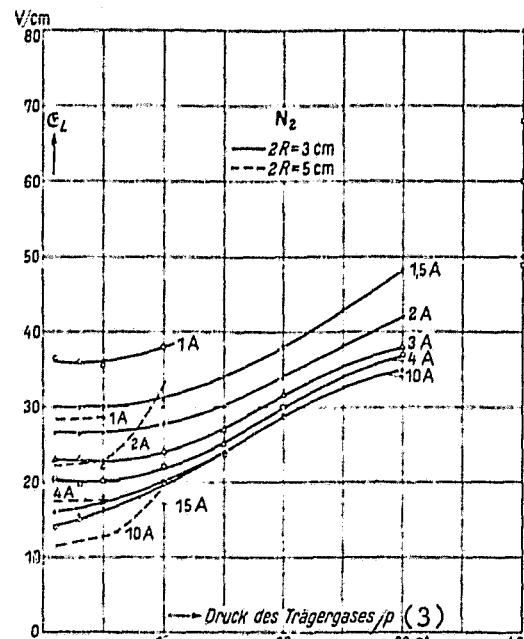


Figure 12 Longitudinal field intensity of rotating arc columns in nitrogen, at 1 to 40 atm and 3 and 5 cm tube diameters, as a function of the current  $i$ .

For each pressure investigated, a family of straight lines as those shown in Figures 8 and 10 were obtained; each of these families produced one curve for the longitudinal field intensity as a function of current. Figure 11 (page 18) shows these curves for all pressures investigated. Correspondingly, the families of straight lines yielded curves for the dependence of the longitudinal field intensity on pressure, with current intensity as the parameter. This family of curves is shown in Figure 12 (page 18).

The two families of curves in Figures 11 and 12 essentially represent the elaboration of all current-voltage characteristics recorded in nitrogen.

Most of the current-voltage characteristics were obtained with a stabilization tube of 3 cm diameter. This stabilization tube was chosen because with it, it was possible

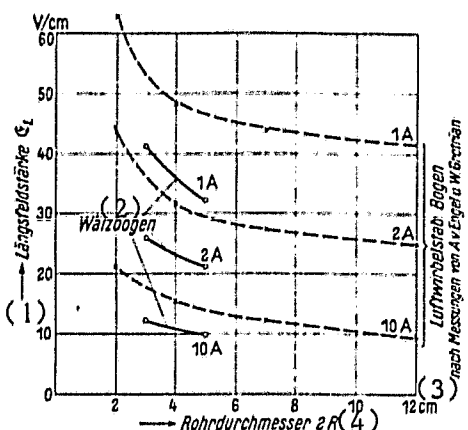
1. to attain better stabilization to higher pressures than with the tube of larger diameter,
2. to have a lower risk of the glass tube shattering, due to the high arc temperatures at greater current intensities, compared to a tube of a smaller diameter.

The 3 cm diameter stabilization tube chosen thus made it possible to encompass a larger range of measurements both with regard to pressure and to current intensity.

However, in order to determine the effect of the tube diameter /38 in the case of rotating arcs - already known and established for air turbulence-stabilized electric arcs - several series of measurements were taken with a stabilizing tube of 5 cm diameter. The results of these measurements, at 1 to 5 atm, are also shown in Figures 11 and 12. At 10 atm, stabilization with the 5 cm tube was no longer possible. It furthermore became apparent that for rotating arcs the tube diameter also affected

the longitudinal field intensity: with increasing tube diameter it decreases in the direction expected, for a given current and pressure.

In order to be able to perform a numerical comparison of the effect of the tube diameter on the longitudinal field intensity in rotating arcs and those stabilized by air turbulence, a measurement series was performed\* also in air, at 1 atm. The results of this measurement series are shown in Figure 13 below



KEY 1 Longitudinal field intensity 2 Rotating arcs 3 Air turbulence stabilized arcs (from A. von Engel and W. Grotrian's measurements)  
4 Tube diameter

Figure 13 Effect of the tube diameter on the longitudinal field intensity of air turbulence-stabilized electric arcs in comparison to rotating arcs, in air at 1 atmosphere

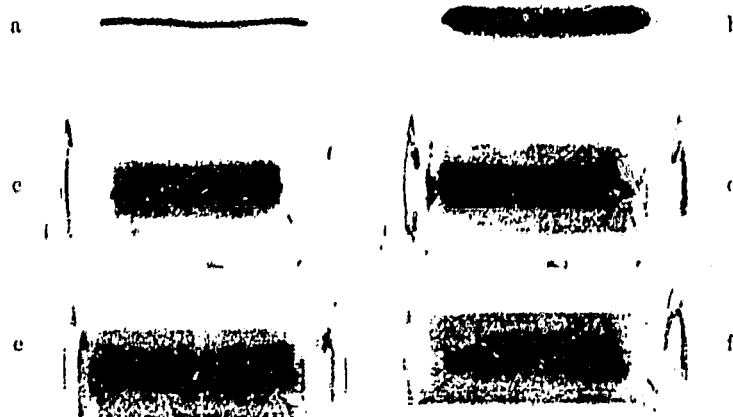
for some current intensities. Simultaneously, this Figure shows A. von Engel's measurement results for air turbulence-stabilized arcs [9], at the same current intensities. The longitudinal field intensity is higher for the air turbulence-stabilized arc by approximately 30%, at all current intensities, in comparison to the rotating arc.

\* We were unable to find any studies of air turbulence stabilized arcs in nitrogen, at various tube diameters, in the literature.

c) Column diameter measurement for current density determinations

Simultaneously with the measurements of the current-voltage characteristics, electric arc photographs were taken to determine the arc diameter. Since for otherwise constant conditions the arc diameter depends only on the current intensity and the pressure - and more especially, is independent of the arc length - it was not necessary to have a photographic record for every measurement point, but only for the different current intensities, at a given pressure. The photographic record - which in the context of current-voltage measurements had to be obtained as rapidly as possible, to include the conditions at the time - was obtained at different arc lengths, depending on the conditions.

The photographs were taken directly on silver bromide paper, with the exposure time, aperture and other adjustments remaining constant. Special efforts were made, in addition, to develop the photographs under the same conditions, in terms of developer composition and development time. Figures 14 and 15, below, show



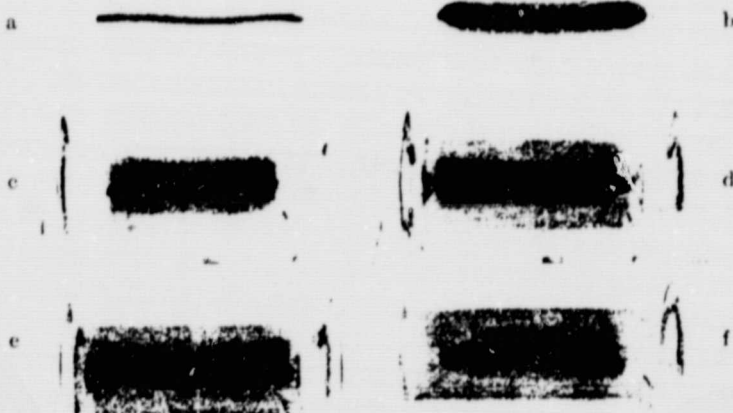
a) 1 atm;  $I = 7$  cm; 0.8 A, c) 1 atm;  $I = 6$  cm; 17 A, e) 15 atm;  $I = 6$  cm; 7.7 A,  
b) 1 atm;  $I = 7$  cm; 5.8 A, d) 5 atm;  $I = 7$  cm; 5.8 A, f) 20 atm;  $I = 6$  cm; 3.6 A.

Figure 14 Photograph of rotating arcs in nitrogen at various pressures.  
Tube diameter:  $2R = 3$  cm

c) Column diameter measurement for current density determinations

Simultaneously with the measurements of the current-voltage characteristics, electric arc photographs were taken to determine the arc diameter. Since for otherwise constant conditions the arc diameter depends only on the current intensity and the pressure - and more especially, is independent of the arc length - it was not necessary to have a photographic record for every measurement point, but only for the different current intensities, at a given pressure. The photographic record - which in the context of current-voltage measurements had to be obtained as rapidly as possible, to include the conditions at the time - was obtained at different arc lengths, depending on the conditions.

The photographs were taken directly on silver bromide paper, with the exposure time, aperture and other adjustments remaining constant. Special efforts were made, in addition, to develop the photographs under the same conditions, in terms of developer composition and development time. Figures 14 and 15, below, show



a) 1 atm;  $l = 7$  cm; 0.8 A, c) 1 atm;  $l = 6$  cm; 17 A, e) 15 atm;  $l = 6$  cm; 7.7 A,  
b) 1 atm;  $l = 7$  cm; 5.8 A, d) 5 atm;  $l = 7$  cm; 5.8 A, f) 20 atm;  $l = 6$  cm; 3.6 A.

Figure 14 Photograph of rotating arcs in nitrogen at various pressures.  
Tube diameter:  $2R = 3$  cm



(1) a) Stickstoff: 30 at;  $I=5$  cm; 4.8 Å; 2 cm Rohrdmr. (3)  
b) Stickstoff: 40 at;  $I=6$  cm; 10.4 Å; 3 cm Dmr. (4)  
c) Stickstoff: 1 at;  $I=7$  cm; 11.7 Å; 5 cm Dmr.  
(2) d) Kohlensäure: 1 at;  $I=6$  cm; 11.4 Å; 5 cm Rohrdmr.,  
e) Kohlensäure: 3 at;  $I=7$  cm; 5.4 Å; 3 cm Rohrdmr.,  
f) Kohlensäure: 10 at;  $I=7$  cm; 3.3 Å; 3 cm Rohrdmr.

KEY 1 Nitrogen 2 Carbon dioxide 3 Tube diameter 4 Diameter

Figure 15 Photographs of rotating arcs in nitrogen and carbon dioxide at various pressures and different tube diameters

some such photographs.

Measurements on the photographs were performed with millimeter-scaled ruler; tenths of millimeters were estimated. In general the diameter was measured at three positions along the columns and then the average was obtained.

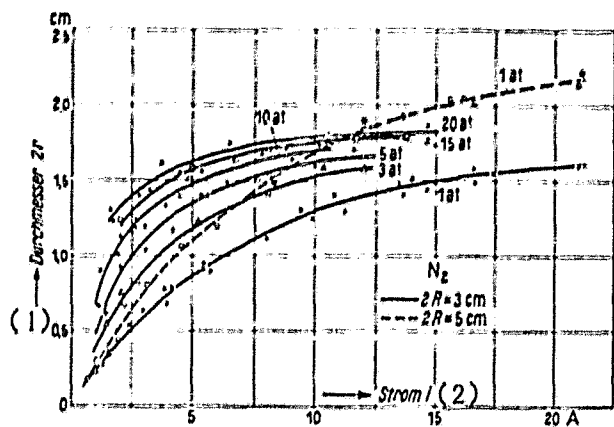
In principle we can state the following, regarding the question of electric arc diameter determinations in nitrogen: the luminous arc column is not sharply delimited towards its edge; rather, the adjoining gas portions - which are of only very limited importance to the current transport along the column [7] - are still relatively luminous; as a consequence, the decrease in luminosity at the arc's edge is less steep than the current density decrease. Hence, in the photographs the intensely black core area must be taken as the arc diameter, which is limited outwards by the first somewhat unsteady decrease in blackness. /39

After some practice, in spite of the undefined edge of the core region it became possible to perform the evaluation within a relatively narrow uncertainty range. It should be pointed out that a more or less intense image of the glass tube is superimposed on the arc picture. The gradually intensifying metal deposit that forms on the inside of the glass tube causes a strong reflection of the arc light - after extended use of the glass cylinder and due to the extraordinarily intense illumination - which in its intensity naturally depends on the arc's current intensity. The now strong diameter increase of the arc column with increasing current density can be readily appreciated in Figures 14a through 14c, for arcs at 1 atm and different current intensities. Figures 14b and 14d show electric arcs at the same current intensity and pressures of 1 and 5 atm, respectively. The remarkable observation can be made, here, that for nitrogen\* the arc column diameter increases, with increasing pressure. For high current intensity arcs, the photographs show that further pressure increases lead to no further recognizable increase in diameter; this is illustrated by Figures 14d and 14e. The arc in Figure 14e has already attained so large a diameter that it fills almost the entire gas space in the glass stabilization tube. An increase in arc diameter is limited by the influence of the stabilization tube, for further pressure and current increases. A comparison of Figures 14f and 15a and 15b illustrates the increased failure of stabilization as the pressure is increased from 20 to 40 atm. /40

Figure 16 (page 24) summarized the column diameters obtained from the photographs of rotating arcs as a function of current intensity, for nitrogen at between 1 and 20 atm. Figure 17 (page 24) is a similar summary for column diameter as a function of pressure. Measurement on photographs at 30 atm and higher was no longer possible, because of the increasing diffusion of the edge, or respectively, no longer made sense due to insufficient

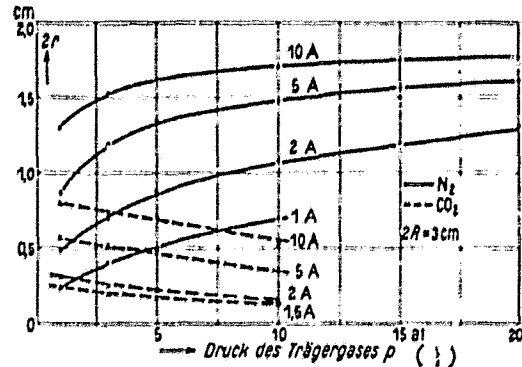
---

\* In contrast to carbon dioxide, as will be shown later



KEY 1 Diameter 2 Current

Figure 16 Rotating arc column diameter at various nitrogen pressures, as a function of the current  $i$



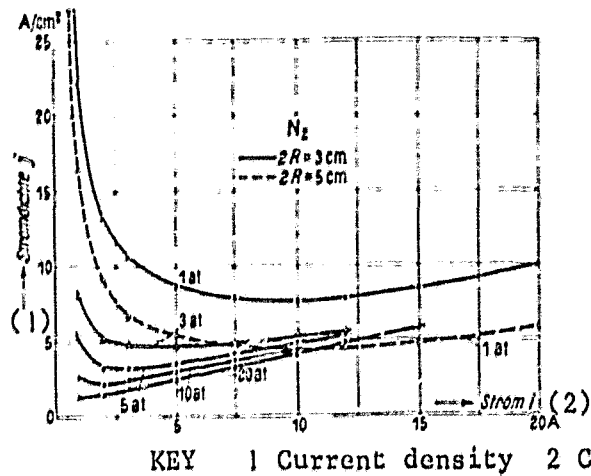
KEY 1 Carrier gas pressure

Figure 17 Column diameter  $2r$  as a function of gas pressure  $p$

stabilization. Numerically, the two families of curves show the increase in arc diameter with increasing current values and at increasing pressures and above all, show clearly that the arc diameter asymptotically approaches a limiting value, which at increasing pressures is attained at ever lower current intensities (Figure 16). At a 5 cm tube diameter this limiting value is larger than at a tube diameter of 3 cm, as can be seen from the broken line curves in Figure 16.

d) Dependence of current density on current intensity, pressure and longitudinal field intensity

The current density  $j$  is obtained from arc radius  $r$  and current intensity  $i$ , as  $j = i/\pi r^2$ , assuming that  $j$  is constant across the arc section. Strictly speaking this assumption is not satisfied, since just as the temperature, the current density gradually decreases, outwardly. But since this decrease in current density is only slight and in addition could not be found in the arc photographs, which were evenly black across the entire diameter, the considerations below were in each case based on the mean current density calculated from the above equation.



KEY 1 Current density 2 Current 3 Pressure

Figure 18 Rotating arc column current density  $j$  as a function of the current  $i$ , in nitrogen at 1-20 atm

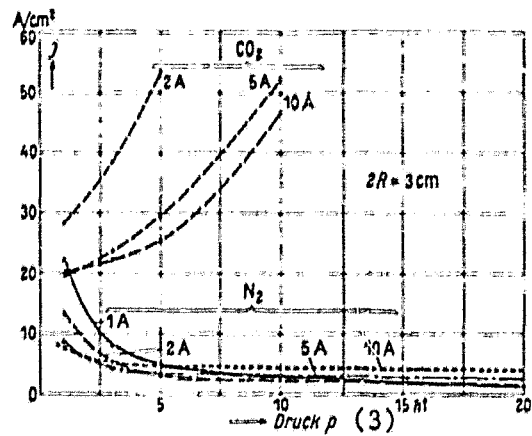
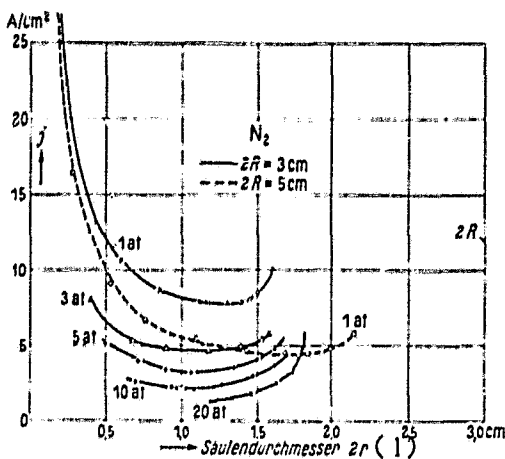


Figure 19 Dependence of current density  $j$  in the rotating arc column on gas pressure  $p$

For better visibility, the current density was not calculated for each individual measurement point, but rather based on the families of curves in Figures 16 and 17; the current density was then plotted as a function of the current, the pressure and the diameter, in Figures 18 and 19, above and Figure 20, below, respectively.

Figure 18 shows that at 1 atm the current density initially decreases steeply, reaches a minimum at approximately 10 A (for a 3 cm tube diameter) and then increases again. This increase in current density is explained by the fact that due to the effect of the stabilizing tube, the arc can not increase its diameter arbitrarily, but that this diameter must approach a limiting value, which at most can equal the stabilization tube's diameter. To the same extent that the arc diameter approaches this limiting value, the increase in current density approaches a limiting value proportional to the current intensity. Without this stabilizing tube influence the current density in the arc column would continuously decrease with increasing current intensity. Naturally, at the 5 cm tube diameter the influence of the tube wall on the arc is smaller. Hence the current density



KEY 1 Column diameter  $2r$

Figure 20 Dependence of current density on column diameter, at various pressures

also decreases to lower values, as shown by the broken line curve in Figure 18. In addition, the current density minimum occurs at greater current intensities (approximately 13 A) than it did for the 3 cm diameter tube.

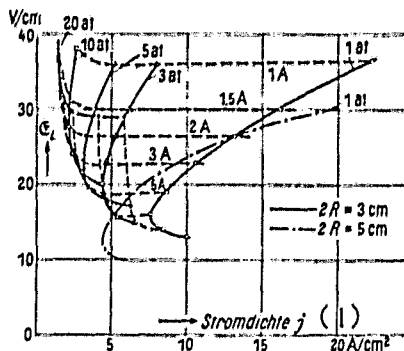
At higher gas pressure, from 3 to 20 atm, in principle the same characteristic course is obtained for the current density as a function of the current, with a marked minimum, as for the 1 atm case. Since as shown above the arc's diameter in nitrogen increases not only for increasing current intensities, but also with increasing pressures, the influence of the stabilization tube on the current density as a function of current is also greater, at higher pressures. This is exteriorized as a shift of the current density minimum towards lower currents (Figure 18). It is also clear, from Figure 18 that at higher pressures - for instance, at 20 atm, for an electric arc - the current density attains unusually low values. For instance, at a current of 2 A the current density is only  $1.5 \text{ A/cm}^2$ . Without the effect /42 of the tube walls, the current density would of course continue to decrease at increasing current intensities, even at this high pressure. It would thus be possible to produce extremely

low current density arcs, in nitrogen. However, they could probably be obtained in a stationary manner only in gravity-free space.

The influence of the stabilization tube on current density is particularly clearly illustrated by the dependence of current density on arc diameter, as shown in Figure 20. Since the arc diameter of an undisturbed arc increases nearly proportionally to the current intensity\*, as shown especially by the curves for 1 atm (tube diameters 3 and 5 cm), the decrease in current density at low arc diameters is approximately inversely proportional to the arc diameter. As the arc diameter increases further, the current density decreases less steeply and attains its minimum at approximately 1 to 1.3 cm diameter, for the 3 cm stabilization tube and at approximately a 1.8 cm diameter for the 5 cm stabilization tube. It is particularly remarkable that this current density minimum occurs at nearly the same column diameter, for all pressures measured; the value of this column diameter is always approximately one third of the tube diameter. The minimum is followed by a steep increase in current density, with the current density apparently approaching a value that is substantially lower than the tube diameter and amounts to only approximately two thirds of the tube diameter. From this it can be concluded that the tube diameter does not affect the column diameter directly, but rather, that the effect of the stabilizing tube must be considered a thermal boundary condition. Even though the stabilization tube is heated by the burning arc, for briefly burning arcs - as in these investigations - it represents a practically constant heat sink with respect to the temperature of the arc column. Hence, an increase in the arc column determines an increase in the temperature gradient from arc to glass tube and hence an increased energy transfer by heat conduction. However, the increase in arc diameter acts as an increase in

---

\* As can incidentally be derived also from the dependence of current density on current intensity



KEY 1 Current density

Figure 21 Dependence of the longitudinal field intensity  $G_L$  on the mean current density  $j$  in the column of a rotating arc in nitrogen at various pressures and current intensities, for  $2R = 3$  cm tube diameter

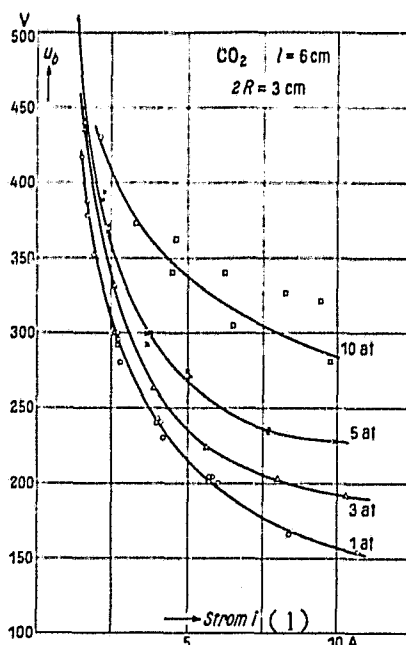
arc cooling, to a greater extent the greater the ratio is between arc diameter and tube diameter. But it is well known that an electric arc reduces its diameter, at increasing cooling [18]. In this context, we shall compare the influence of the stabilization tube in the rotating arc here investigated, and that on the air turbulence-stabilized arc. According to A. von Engel [9], the minimum of the current density for an air turbulence-stabilized arc at 1 atm lies near one tenth of the tube diameter. Thus, the influence of stabilization is substantially higher than for rotating arcs, which is as expected, in the light of the preceding considerations, since in that case the energy removal from the arc column - i.e., arc cooling - occurs not only by heat conduction, but primarily by convection, through the stabilizing gas masses of the air turbulence. /43

If the longitudinal field intensities are plotted as a function of the current density, as in Figure 21, above, then each point represents one value of the mean output density in the arc column. Lines of equal output density are described by equilateral hyperbolas. The measurement values plotted in the graph for equal carrier gas pressures show an unusual course. It is remarkable that they have a common unilateral osculating curve, whose course approximately overlaps that of an equilateral

hyperbola, i.e., a line of equal output density. But this means that the columns output density at different pressures and current intensities can not fall below a certain limiting value. This limiting value depends on the tube diameter, however, as can be seen from the equally plotted curve for the 5 cm stabilization tube at 1 atm; at increasing tube diameters it becomes displaced towards the lower values.

If the output density is plotted as a function of pressure, with the arc diameter as parameter, then for diameters between 0.5 and 1.3 we obtain a family of decreasing characteristics, which at high pressures approach a lower limiting value.

## 2. Measurements in Carbon Dioxide

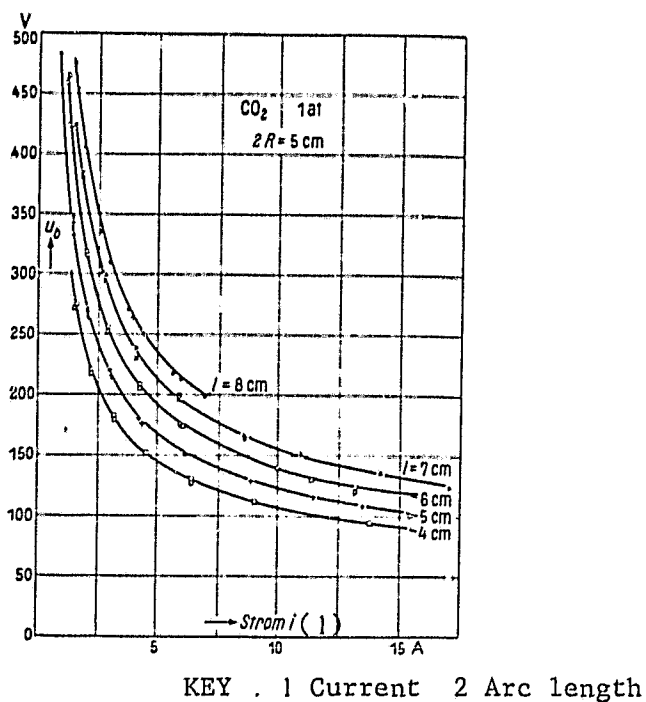


KEY 1 Current

Figure 22 Current-voltage characteristics of rotating arcs of constant length, in carbon dioxide at 1 to 10 atmospheres

The measurements were performed in carbon dioxide just as in the investigation with nitrogen; the evaluation and elaboration

ORIGINAL PAGE IS  
OF POOR QUALITY



KEY . 1 Current 2 Arc length

Figure 23 Current-voltage characteristics of rotating arcs of different lengths, in carbon dioxide at 1 atm

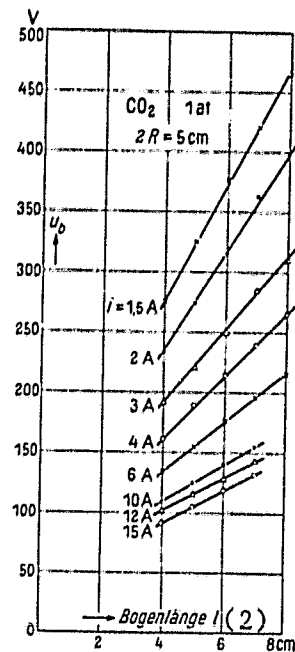


Figure 24 Arc voltage  $U_b$  as a function of arc length  $l$ , in carbon dioxide at 1 atm

of the measurement results was also similar.

a) Current-voltage characteristics and longitudinal field intensity

The current-voltage characteristics shown in Figure 22 (page 29) for carbon dioxide at various pressures (arc length 6 cm, stabilization tube 3 cm diameter) depart from those obtained for nitrogen under otherwise equal conditions (Figure 6) both in their absolute values and in their course. In carbon dioxide the arc voltage is higher than in nitrogen, for the same current and pressure, and decreases more steeply with increasing current than it does in nitrogen.

Figures 23 and 24, above, show the determination of the longitudinal field intensity, for carbon dioxide at 1 atm, to indicate /44

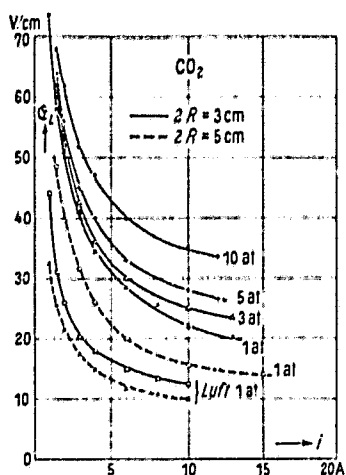


Figure 25 Longitudinal field intensity of rotating arc columns in carbon dioxide at various pressures and tube diameters, as a function of the current intensity  $i$

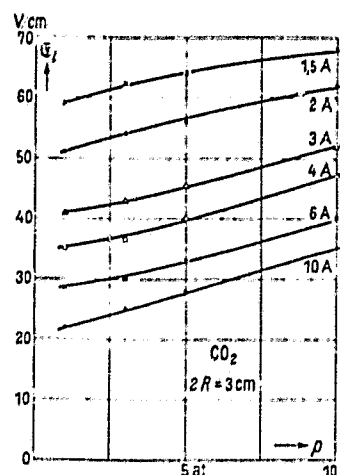


Figure 26 Longitudinal field intensity of rotating arc columns in carbon dioxide, as a function of the pressure  $p$ , for various current intensities

that the longitudinal field intensity is also constant, in the investigated range of arc columns. Provided the columns were stabilized, this constancy occurred also at higher pressures.

Figures 25 and 26, above, show the dependence on current intensity and pressure, respectively, of the longitudinal field intensity in carbon dioxide. A comparison between Figure 25 and the corresponding curves for nitrogen (Figure 11) shows that at equal pressures and currents the longitudinal field intensity is higher in carbon dioxide than in nitrogen, in all cases, with a value almost twice as high.

Example:  $N_2$  at 1 atm, 2A,  $E = 26.5$  V/cm; at 10 atm, 2A,  $E = 27.5$  V/cm  
 $CO_2$  at " "  $E = 51$  V/cm; " " "  $E = 62$  V/cm

In addition and with regard to the pressure dependence of the longitudinal field intensity, the arc in carbon dioxide shows a different behavior than in nitrogen, as a comparison of Figures 12 and 26 shows. While in nitrogen the longitudinal field intensity remains constant up to 5 atm, at low currents, or even

decreases, to only increase later, in carbon dioxide the longitudinal field intensity already increases after 1 atm, with a nearly linear increase over the pressure range studied. This discovery is especially remarkable because for the carbon dioxide arc studied we are dealing with a range in which edge distortions due to the stabilizing tube are of subordinate importance, for carbon dioxide much more so\* than for nitrogen.

Figure 25 shows, in addition, the longitudinal field intensity as a function of current intensity for a stabilization tube of a 5 cm diameter. The influence of the greater tube diameter can be seen also here in the decrease of the longitudinal field intensity.

b) Column diameter and current density

/45

It is already known from W. Grotrian's studies that an electric arc in carbon dioxide at 1 atm looks different from an arc in nitrogen (or air). Under otherwise equal conditions, the arc column in carbon dioxide is more sharply delimited, of a smaller diameter, whiter and more luminous than in nitrogen. The rotating arc in carbon dioxide here investigated showed this different behavior in comparison to nitrogen also at higher pressures, as shown by a comparison of the arc photographs for the two gases (Figures 14 and 15).

The determination of the arc diameter from the photographs was simpler to perform, because of the sharper edges, in carbon dioxide, than it had been in nitrogen. While for nitrogen stabilization was possible up to 20 atm, the arc in carbon dioxide could be kept stable only to 8 atm. Stabilization was already slightly disturbed at 10 atm, as shown in Figure 15f; at 15 atm stabilization had already failed entirely.

---

\* Due to the smaller arc diameter, in carbon dioxide.

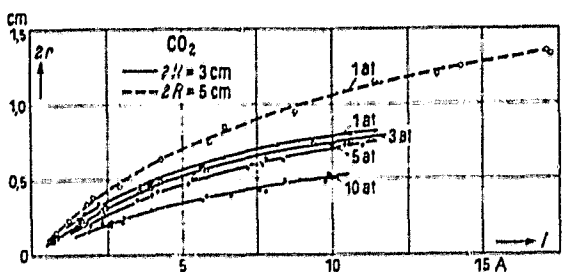


Figure 27 Column diameter  $2R$  of a rotating arc in carbon dioxide at various pressures, as a function of current

In Figure 27, above, the column diameter obtained from photographs is plotted as a function of the current. Naturally, the column diameter increases with increasing current. While the arc voltage and the longitudinal field intensity in carbon dioxide show certain departures in their pressure dependence in comparison to nitrogen, the pressure dependence of the diameter in carbon dioxide and in nitrogen is nearly opposite. While in nitrogen the arc diameter increases with increasing pressure (Figure 16), it decreases in carbon dioxide (see also Figure 17, in the pressure dependence of the diameter, shown jointly for carbon dioxide and nitrogen). Figure 17 provides a numerical ration of the arc diameters (nitrogen to carbon dioxide) of approximately 1.6 at a 1 atm pressure. This ratio is independent of current intensity. At higher pressures it increases more steeply, the smaller the current intensity is. It has a value of 6.7, for instance, at 10 atm and 2A, but a value of 3.1 at 10 atm and 10A. The fact that at higher pressures this diameter ratio decreases with increasing currents can probably be explained in terms of the increasing influence of the edge, in nitrogen. /46

The current density, plotted in Figure 28 (page 34) as a function of current intensity, initially decreases for all pressures at increasing currents, attaining a minimum, as for nitrogen (Figure 18). This minimum is attained, at all pressures, at an arc diameter approximately one fourth of the tube diameter.

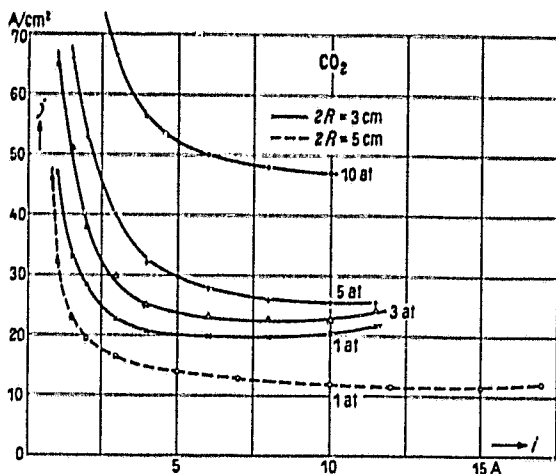


Figure 28 Current density in the column of a rotating arc in carbon dioxide at different pressures as a function of the current  $i$

In contrast to nitrogen, in carbon dioxide the current density increases with increasing pressure, as can be seen in Figure 19.

## V COMPARISON BETWEEN MEASUREMENT RESULTS AND THEORY

### a) Arc column conductivity in nitrogen

The current density in the column of an arc discharge is expressed in K. T. Compton's thermal arc theory [22] by the equation

$$j = \epsilon \cdot n^- \cdot v^- = \epsilon \cdot n^- \cdot b^- \cdot \mathfrak{E}, \quad (1)$$

where  $\epsilon$  is the elementary electric charge,

$n^-$  is the number of electrons per  $\text{cm}^3$ ,

$v^-$  is the mean diffusion velocity of the electron,

$b^-$  is the electron mobility, and

$\mathfrak{E}$  is the driving field intensity\*

\* Strictly speaking equation (1) does not include the entire current density, but only that produced by the electrons as

The number of electrons  $n^-$  can be calculated, from the equation

$$\frac{x^2}{1-x^2} \cdot p = 2.4 \cdot 10^{-4} \cdot T^{1.25} \cdot e^{\frac{V_j}{k \cdot T}} \quad (2)$$

given by Megh Nad Saha for the degree of ionization  $x^{**}$ , as a function of temperature and pressure, as

/47

$$n^- = x \cdot N. \quad (3)$$

where  $N$  is the number of neutral molecules or atoms, respectively, existing prior to thermal ionization,

$p$  is the gas pressure in mm Hg,

$T$  is the absolute temperature of the arc column, in  $^{\circ}\text{K}$ ,

$k$  is Boltzmann's constant, and

$V_j$  the carrier gas' ionization potential

Since the degree of ionization  $x$  for nitrogen, under the temperature conditions present in the rotating arc - approximately  $5000^{\circ}\text{K}$  - is a very small quantity, equation (2) can be written

$$x = \text{const} \cdot g_x(T) \cdot p^{-1/2}, \quad (4)$$

where the temperature terms are combined in  $g_x(T)$ .

The quantity  $N$  of neutral molecules is directly proportional to the gas pressure and hence we obtain the following expression for the pressure dependence of the number of electrons per unit volume in the arc column:

---

(continued from previous page) charge carriers, while the current density caused by the equal number of ions present is not taken into consideration. As is known, this approximation is permissible because the mobility of the ions - and hence, their diffusion velocity - is so much smaller than that of the electrons, that their contribution to the current density is negligible.

\*\* The calculation of the degree of ionization  $X$  by the Saha equation is possible only as an approximation, since the existence, or respectively, the occurrence of excited states is neglected, i.e., direct ionization is assumed, without intermediate stages; in addition, molecular vibrations are also neglected, among other things.

$$n = \text{const} \cdot g_n(T) \cdot p^{1/2}, \quad (5)$$

The electron mobility  $b$  [equation (1)] is also pressure dependent, since as is known, it is given by the expression

$$b = \frac{e}{13 \cdot \mu \cdot k} \cdot \frac{\lambda}{T}$$

( $\mu$  = mass of the electron). The mean free path of the electrons  $\lambda$  is inversely proportional to the gas pressure and hence

$$b \approx \frac{1}{p}. \quad (6)$$

We now obtain the following expression for the pressure dependence of the specific conductivity of the arc column,  $\sigma_{\text{arc}}$ , from equations (1), (5) and (6)

$$\sigma_{\text{arc}} = n \cdot e \cdot b \approx \text{const} \cdot g(T) \cdot p^{-1/2}. \quad (7)$$

In the derivation of equation (7) we assumed that the ionization potential  $V_j$  in Saha's equation (2) is independent of the gas pressure. While this is true of monoatomic gases, it does not apply to the molecular gases nitrogen and carbon dioxide here investigated.

In the arc column the nitrogen molecules  $N_2$  and the nitrogen atoms  $N$  are partially dissociated\* according to  $N_2 \rightleftharpoons N$ , as a function of gas pressure and temperature, where the degree of dissociation is given by the equation

$$\log \frac{4z^2}{1-z^2} \cdot p = - \frac{5040}{T} W + \frac{3}{2} \log T + 0,442 - \log V(T). \quad (8)$$

where  $W$  is the dissociation energy ( $W = 7.4V$  for nitrogen),  $V(T)$  is the equation of state for  $N_2$  molecule vibrations,  $p$  is the gas pressure, in atm

---

\* While the following considerations and calculations apply to nitrogen, they can in principle be extended to carbon dioxide

If in equation (8) we make the temperature constant, then we obtain, with sufficient precision,  $\approx p^{-1/2}$ . For a temperature of 5000°K, which approximately corresponds to the rotating arc temperature in nitrogen, we obtain the following numerical values of the degree of dissociation  $z$  of nitrogen, at the pressures indicated:

$p$	1	5	10	20 at
$z$	0,070	0,035	0,025	0,018

The ionization potential  $V_j$  of nitrogen molecules is 15.8 V, but that of nitrogen atoms is only 14.5 V. Thus, at higher pressures there will be fewer of the more readily ionizable nitrogen atoms present than at lower pressures, i.e., the resulting ionization potential  $V_j$  res will be lower for the mixture  $N_2 + 2N$  at increasing pressures and hence, according to equation (2), so will be the resulting degree of ionization,  $x_{res}$ .

If the resulting degree of ionization  $x_{res}$  is calculated numerically as a function of pressure - where a system of equations must take into account that atomic nitrogen is more strongly ionized by lower ionization work than corresponds to the percentual proportion determined by thermal dissociation of molecular nitrogen - then we obtain the rounded values shown in the table below:

$p$ at	1	5	10	20
$x_{res} \cdot p^{1/2}$	$75 \cdot 10^{-6}$	$50 \cdot 10^{-6}$	$44 \cdot 10^{-6}$	$40 \cdot 10^{-6}$

This additional decrease in the resulting ionization potential  $x_{res} \cdot p^{1/2}$  as a function of pressure, caused by the decrease in the degree of dissociation of  $N_2$ , can be equated to the following power ranges of the pressure:  $x_{res} \cdot p^{1/2} \approx p^{-1/6}$  to  $p^{-1/4}$ . Taking this into consideration, equation (7) yields the following expression for the specific conductivity of the rotating nitrogen arc:

$$\frac{J}{\ell} = n \cdot e \cdot b = \text{const} \cdot g(T) \cdot [p^{-2/3} \text{ to } p^{-3/4}]. \quad (9)$$

In subsequent considerations, for reasons of simplicity only one power shall be used,  $p^{-3/4}$ .

This equation will be used in the comparison with measurement results. It must be taken into consideration, here, that no statement can be made regarding the pressure dependence of the temperature function  $g(T)$ , since the temperature in the electric arc was not measured, in this investigation. In order to allow the comparison, we shall assume constant temperature, initially, in equation (9). We thus obtain

$$\frac{j}{\sigma} = \text{const} \cdot p^{-3/4}. \quad (10)$$

Based on the expectation that the assumption of constant arc temperature would more readily be satisfied by rotating arcs of equal column diameter, the specific conductivity was determined as a function of pressure for equal column diameters, from the curves in Figures 11, 16 and 20, and plotted in Figure 29 below:

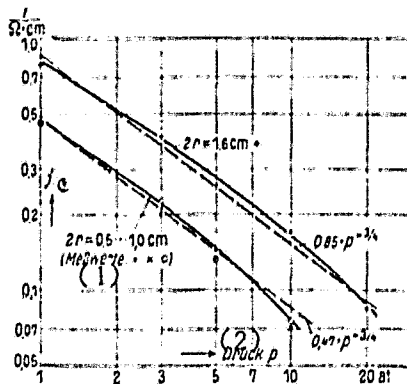


Figure 29 Comparison between experimentally obtained and calculated courses of the conductivity  $j/\sigma$  in the arc column in nitrogen, as a function of pressure. Tube diameter 3 cm (2r = arc diameter)

The same Figure also shows the course of the theoretically determined pressure dependence of the specific conductivity, expressed by equation (10), both for small column diameters

$2r = 0.5$  to  $1.0$  cm and for  $1.6$  cm diameters. Thus, the constant in equation (10) was not calculated, but resulted from the adaptation of the experimental values.

The agreement between the calculated and the experimentally determined curves, in Figure 29, is surprisingly good. This also indicates that the assumption of constant arc temperature for equal arc column diameters, at increasing pressure, is accurate within certain limits. /49

The temperature function  $g(T)$  in equation (9) can be calculated numerically for various temperatures, from equations (2) and (5). For the temperature range from  $4000^{\circ}\text{K}$  to  $7000^{\circ}\text{K}$  one obtains the approximation  $\pi(T) \approx T^{1.5}$  to  $T^{2.0}$ . Correspondingly, at  $5000^{\circ}\text{K}$ , for instance, a temperature increase of only 10% determines an increase in the specific conductivity by a factor of 4 to 7 (at 5%, a 2 to 3-fold increase). Thus, if for a gas pressure increasing from 1 to 20 atm the arc temperature had changed by as little as 10%, the good agreement shown by the curves in Figure 29 would not have been possible. One must conclude, rather, that at least for equal column diameters the temperature remained constant within a few percent, for the pressure range of 1 to 20 atm.

Figure 29 furthermore shows that the specific conductivity increases with increasing column diameter (0.5-1.0 and 1.6, respectively), but that the pressure dependence of the specific conductivity  $\pi$  can be adequately described by equation (10) for any column diameter. From this we may conclude that the arc temperature of a rotating arc in nitrogen depends only on the column diameter, within narrow limits, with the arc temperature increasing with increasing column diameter. It is assumed that this temperature increase is caused by edge effect influence of the stabilization tube, which increases with increasing column diameter (gradual constriction of the arc column, which leads to increased arc cooling).

b) Arc column energy in nitrogen

In a rotating arc, the energy absorbed by a 1 cm length of arc column,  $\mathfrak{G} \cdot i$ , is eliminated almost exclusively by heat conduction. The proportion of energy released by radiation is only approximately 10%, according to measurements performed on a freely burning arc at 20A, and according to calculations for a stabilized electric arc. It will therefore be neglected, during the considerations to follow\*.

Hence the following energy equation applies to rotating arcs:

$$\mathfrak{G} \cdot i = \frac{2\pi}{\ln \frac{R}{r}} \int_{T_0}^T \lambda dT. \quad (11)$$

where  $R$  is the radius of the stabilization tube with the approximately constant temperature  $T_0$ ,  
 $r$  is the radius of the arc column, at mean temperature  $T$ ,  
 $\lambda$  is the thermal conductivity\*\*.

We shall now consider the experimentally determined pressure dependence of the energy absorbed by the arc, in nitrogen, on the basis of the above equation.

The experimental values of  $\mathfrak{G} \cdot i$  can be derived from the families of curves in Figures 11 and 16. It is optional to keep one of the experimental magnitudes constant, here. It is advantageous

\* There is no energy release by convection cooling, in rotating arcs (provided stabilization is unobjectionable).

\*\* This equation was derived for an incandescent rod of diameter  $2r$ , with a surface temperature  $T$ , placed in a tube of diameter  $2R$  at a constant temperature  $T_0$ . Since the arc does not have a sharply defined edge at which the temperature is  $T$  - as already mentioned in section 4c and 4d, respectively - also here only a mean temperature can be postulated, for a mean arc radius  $r$ . The small changes in the supposedly constant temperature  $T_0$  of the stabilization tube have only a small effect on changes in energy release, because of the low thermal conductivity at the occurring temperature of  $T_0$ , between 300°K and 400°K.

UNSTABILIZED  
OF POOR QUALITY

to keep the arc radius constant, since in that case the arc temperature also remains constant, is discussed in the previous section. The right side of the energy equation is greatly simplified thereby, and we obtain

$$(\mathcal{E} \cdot i)_{r=\text{const.}} = \text{const.} \cdot \lambda = f(p). \quad (12)$$

The energy  $\mathcal{E} \cdot i$  is shown in Figure 30, below for various radii  $r$ ,

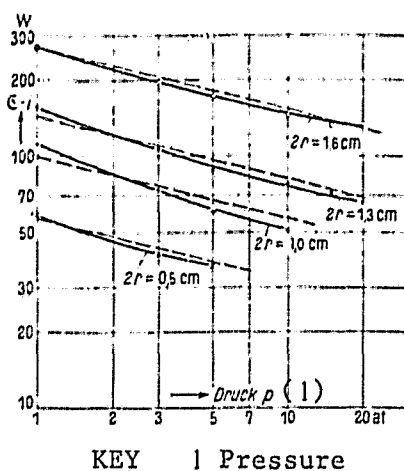


Figure 30 Energy of an arc column in nitrogen as a function of pressure. From measurements and calculations using  $\lambda \approx p^{-1/4}$  ( $2r$  = arc diameter)

as a function of pressure. Figure 30 shows a family of curves of decreasing characteristics. As the arc radius increases, the curves become displaced towards the higher energies. If equation (12) is valid, according to their course these curves should be described by the function  $\lambda = f(p)$ . This shall be examined below.

As long as thermal dissociation is negligible - i.e., within the range of low and intermediate temperatures - the thermal conductivity coefficient  $\lambda$  of gases is independent of pressure\*.

\* We have  $\lambda = K \cdot \mu \cdot c_v$ , where  $K = \text{const.}$ ,  $\mu = \text{viscosity}$ ,  $c_v = \text{specific heat}$ ;  $c_v$  is independent of gas pressure. Furthermore, we have  $\mu = 1/3 \cdot \rho \cdot u \cdot L$ , where  $\rho = \text{density}$ ,  $u = \text{velocity of the molecules}$ ,  $L = \text{mean free path length}$ . Since both  $u$  and the product  $\rho \cdot L$  are pressure independent, so are  $\mu$  and hence  $\lambda$ .

However, within the range of thermal dissociation  $\lambda$  becomes pressure dependent, because

1. The equilibrium  $N_2 \rightleftharpoons 2N$  is displaced and  $\lambda$  is different for  $N_2$  and for  $N$ , and
2. there is an additional heat transfer due to the dissociations and recombinations taking place at different sites.

The increase in the thermal conductivity coefficient  $\lambda_x$ , determined only by the second process, is described by W. Nernst by means of the equation

$$\lambda_x = -D \cdot W \cdot \frac{d\rho}{dz} \cdot \frac{dz}{dT},$$

where  $D$  is the diffusion constant,  
 $W$  is the dissociation energy in V (for  $N_2 \rightleftharpoons 2N$  it is  $W = 7.4$  V),  
 $\rho$  is the number of molecules per unit volume, and  
 $z$  is the degree of dissociation.

Using this equation, according to calculations by Ter Horst, /51 H. Brinkmann and L. G. Ornstein [24], the following equation is obtained for the pressure dependence of the thermal conductivity coefficient  $\lambda$  for nitrogen, at constant temperature:

$$\lambda = K_1 \frac{2z}{1+z} + K_2 \frac{1-z}{1+z} + \lambda_x. \quad (13)$$

The first times indicates the fraction of the thermal conductivity coefficient due to the atoms, the second term that due to molecules. For nitrogen at constant temperature, we have

$$\lambda_x = K_3 \left[ \frac{1^2}{18 \frac{z}{1-z} + 17,5} + \frac{1}{18 \frac{1-z}{z} + 24,7} \right] \frac{W}{(1+z)^2} \cdot x. \quad (14)$$

where  $K_1 \dots K_3$  are constants.

$\lambda = f(p)$  was calculated for 5000°K from equations (13) and (14) and the values of  $z$  given above for various pressures. The numerical values obtained can be adequately described by

$$\lambda \approx p^{-1/4} \quad (15)$$

for the pressure range of 1 to 20 atmospheres.

Next, in Figure 30 (page 41) a curve  $\lambda = \text{const} \cdot p^{-1/4}$  was drawn for each column diameter, equated to the corresponding experimental value of  $\mathfrak{E} \cdot i$ . The agreement between the curves  $\lambda \approx p^{-1/4}$  and the experimental  $\mathfrak{E} \cdot i$ -values must be viewed as quite good. From this we can conclude that the application of the energy equation to the rotating arcs is justified and consider the agreement observed as further proof that the temperature in the arc column is practically independent of pressure, at constant arc diameter.

By means of energy equation (11) it is now also possible to provide an explanation for the course of the longitudinal field intensity in nitrogen, for constant current and as a function of pressure, as shown in Figure 12 and already discussed. Let us consider the field intensity for 2 A. In the range of 1 to 7 atm,  $\mathfrak{E}$  remains approximately constant and then increases regularly with increasing pressure. It can be seen from Figure 17 that for 2A, the arc diameter also increases with increasing pressure. The dependence of the arc radius  $r$  on pressure can be described approximately by

$$\ln \frac{1}{r} \approx p^{-1/4}.$$

according to Figure 17.

As shown in the previous section, the arc temperature is constant\* to arc diameters of approximately 1 cm.

---

\* Obviously this applies only to the conditions discussed,  $N_2$  as carrier gas and a 3 cm diameter stabilization tube

Hence, for this range the energy equation can be written

$$\mathfrak{E} \cdot i = \frac{2\pi}{\ln \frac{R}{r}} \cdot \lambda(p) = \text{const} \cdot p^{1/4} \cdot p^{-1/4} = \text{const} \quad (16)$$

or

$$\mathfrak{E}(p)_{i=\text{const}} = \text{const}, \quad (17)$$

i.e., for the pressure range just mentioned and a current of 2A, using the energy equation we obtain a pressure independent course for the longitudinal field intensity, just as it was measured.

For higher pressures, i.e., greater arc radii, the temperature no longer remains constant, but gradually increases, which is also reflected in an increasing longitudinal field intensity  $\mathfrak{E}$ .

c) Current and pressure dependence of the longitudinal field intensity, according to the "minimum principle"

While in the two preceding sections - V a) and V b) - combined measurement values were used for comparisons with analytically determined relationships, we shall now theoretically determine the current and especially, the pressure dependence of the arc column's 3 dependent variables  $\mathfrak{E}$ ,  $r$  and  $T$ , individually, and compare them to measurement results.

In addition to the two previously discussed equations (1) and (11) for the conductivity and energy of the arc column, respectively, we shall now use a third equation, from the theory of the lowest burning voltage, already used several times elsewhere, in this context [18-20]. According to this minimum theory, the arc column's temperature and diameter mutually adjust in such a manner that at a given current the electrode voltage - or the longitudinal field intensity, respectively - becomes a minimum:

$$\frac{d\mathfrak{E}}{dT_{i=\text{const}}} = 0^1). \quad (18)$$

a) First we shall examine the dependence on the current of the rotating arc's longitudinal field intensity:  $\mathfrak{E} \cdot /i$ . To this end we shall return to equation (9) for the arc column's conductivity and rewrite for constant pressure, in the form

$$i = n \cdot \epsilon \cdot b \cdot \mathfrak{E} \cdot \pi \cdot r^2 = \text{const} \cdot g(T) \cdot r^2 \cdot \mathfrak{E}. \quad (19)$$

In addition, we shall need the energy equation (11)

$$\mathfrak{E} \cdot i = \frac{2\pi}{\ln \frac{R}{r}} \int_{r_0}^T \lambda dT.$$

If we want to eliminate  $r$  from these two equations, then we must approximate the logarithmic term by means of a power  $m$  of  $r$ , since otherwise we shall encounter unsurmountable difficulties in the course of subsequent calculations. We shall thus use

$$\mathfrak{E} \cdot i = r^m \cdot f(T); \quad (20)$$

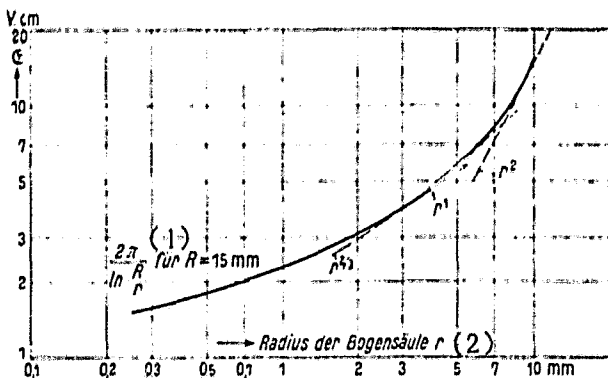
eliminating  $r$ , we obtain

$$i^{m-1} \cdot \mathfrak{E}^{m-1} = \text{const} \frac{[f(T)]^{\frac{2}{m}}}{g(T)}. \quad (21)$$

The determination of  $m$  is accomplished graphically.

In Figure 31 (page 46),  $\frac{2\pi}{\ln \frac{R}{r}}$  is plotted as a function of the arc radius  $r$ , for a stabilizing tube of  $R = 15$  mm. For an arc radius of 2 to approximately 4 mm, which for nitrogen at 1 atm /53 corresponds to an arc current of 2 to 4.5 A, according to Figure 16,  $\frac{2\pi}{\ln \frac{R}{r}}$  can be approximated by  $r^{4/3}$ , as shown in Figure 31. For this current range  $m$  is hence = 2/3 and equation (21) becomes

$$i^2 \cdot \mathfrak{E}^4 = \frac{[f(T)]^3}{g(T)}. \quad (22)$$



KEY 1 für = for 2 Arc column radius

Figure 31 Replacement of  $\frac{2\pi}{\ln \frac{R}{r}}$  by powers of  $r$

This equation, differentiated with respect to  $T$  corresponding to the extreme condition (18), yields

$$i^2 \cdot \mathfrak{G}^4 = \frac{d}{dT} \left[ \frac{[f(T)]^3}{g(T)} \right] = 0$$

which resolves to

$$i^2 \cdot \mathfrak{G}^4 = \text{const};$$

or

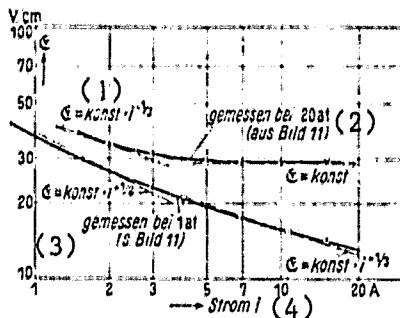
$$\mathfrak{G} = \frac{\text{const.}}{i^2}. \quad (23)$$

For an arc radius of approximately 5 to 7 mm, it is possible - as can be seen from Figure 31 - to approximate  $\frac{2\pi}{\ln \frac{R}{r}}$  by  $r^1$ . For these limits of the column diameter (10-14 mm), at 1 atm we derive a current range of approximately 6-12 A, from Figure 16. If in equation (21) we set  $m = 1$  and perform the calculations and the derivation with respect to  $T$  as above, then we obtain, for the current range just mentioned,

$$\mathfrak{G} = \frac{\text{const.}}{i^3}. \quad (24)$$

These analytically determined current dependences of the longitudinal field intensity after equations (23) and (24) are

ORIGINAL DRAWING  
OF POOR QUALITY



KEY 1 konst. = constant 2 Measured at 20 atm (from Figure 11) 3 Measured at 1 atm (see Figure 11)  
4 Current

Figure 32 Comparison of measurement results and theory.  $E = /i^{1/2}$  at 1 and 20 atm for nitrogen and 3 cm tube diameter

are plotted in Figure 32, above, together with the measured values, at 1 atm and 2 or 10 A, respectively.

Thus, not absolute values but the course of the longitudinal field intensity - of greatest interest - is shown, here.

Figure 32 shows clearly that the nature of the measured current-voltage curves can be substantially adequately described by the course calculated with the aid of the minimum principle. It is clear that the agreement can only be rough, since the approximation of the logarithmic expression by means of powers of  $r$  is possible precisely only at one point, in each case.

In a similar manner we shall also calculate the current dependence of the longitudinal field intensity in nitrogen at 20 atm.

According to Figure 16, for a current range of 1.5 to 3 A the arc diameter lies between 12 and 14.6 mm, i.e., the radius between 6 and 7.3 mm. For this range of radii we already performed the approximation. We obtained equation (24):  $E = \frac{\text{const}}{i^{1/2}}$ . For the current range of 5 to 15 A, from Figures 16 and 31 and corresponding to  $m = 2$ , we obtain

$$E = \text{const.} \quad (25)$$

Figure 32 also shows the measured and calculated curves at 20 atm. Once again, the calculated values were approximated for comparison to the measured values at 2 and 10 A, respectively. The agreement still is surprisingly good, even though the assumption of energy release exclusively by heat conduction becomes less and less valid, especially at the larger currents and column diameters, because of the increasing proportion of radiative heat loss.

β)  $\mathfrak{E} = f(p)$ ; pressure dependence of the longitudinal field intensity. Once again we shall use equations (1) and (11), however taking  $p$  into account [equations (9) and (16)]

$$i = n \cdot \epsilon b \cdot \mathfrak{E} \pi \cdot r^2 = \text{const} \cdot g(T) \cdot r^2 \cdot \mathfrak{E} \cdot p^{-1/4} \quad (26a)$$

and

$$\mathfrak{E} \cdot i = \text{const} \cdot r^m \cdot f(T) \cdot p^{-1/4}. \quad (26b)$$

Eliminating  $r$ , we obtain

$$i^{\frac{2}{m}-1} \cdot (\mathfrak{E}^{m+1} \cdot p^{2m-3})^{\frac{1}{4}} = \text{const} \frac{[f(T)]^m}{g(T)}. \quad (26c)$$

It can be seen from Figure 17 that for the pressure range of 1 to 5 atm the arc diameter for nitrogen at 2 A lies between 0.5 and 0.9 mm. According to Figure 31 we obtain, as an approximation,  $\frac{2\pi}{\ln R} = \text{const} \cdot r^{1/2}$ . If in equation (26) we set  $m = 1/2$  and differentiate with respect to  $T$  as above, we obtain

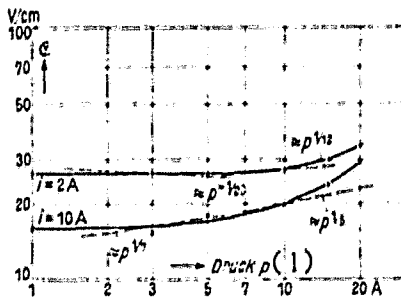
$$i^3 \cdot \mathfrak{E}^5 \cdot p^{1/4} = \text{const},$$

or as a pressure dependence of the longitudinal field intensity at constant current,

$$\mathfrak{E} \approx p^{-1/20}. \quad (27)$$

In a similar manner we obtain, for 2 A and a pressure range of 10 to 20 atm,  $m =$  approximately 1 and hence  $\mathfrak{E} \approx p^{1/12}$ ; for 10 A and a pressure range of 1 to 5 atm,  $m = 4/3$  and thus  $\mathfrak{E} \approx p^{17/12}$ ; for 10 A and the pressure range 5-20 atm,  $m = 5/3$  and  $\mathfrak{E} \approx p^{15/12}$ .

ORIGINAL PAGE IS  
OF POOR QUALITY



KEY | Pressure

Figure 33 Comparison of measurement results according to Figure 12 and the minimum theory.  $E = f(p)$  for  $N_2$  and  $2R = 3 \text{ cm}$

This theoretically determined course of the pressure dependence is shown in Figure 33, above, together with the measured values. Once again, the calculated curves were approximated to the measured ones, at 3 and 10 atm.

It is especially interesting that according to the minimum principle at low current intensities (2A) a decrease occurs in the longitudinal field intensity, at increasing pressure, between 1 and 5 atm. As Figure 12 shows, in some cases such a decrease was actually measured.

At higher current intensities and pressures the theoretical curve significantly deviates from the experimental one, for the reasons already mentioned (especially, increase in energy loss by radiation, here not taken into account).

d) Column diameter and column temperature pressure dependence /55 according to the minimum principle

a)  $r = f(p)$ . From the two equations (26) and (26a) shown on page 48, eliminating  $E$  we obtain for the column radius  $r$ :

$$r = \frac{i^{m+2} \cdot p^{\frac{1}{m+2}}}{f(T)^{m+2} \cdot g(T)^{\frac{1}{m+2}}}, \quad (28)$$

or respectively, for constant current and assuming constant temperature:

$$r = \text{const} \cdot p^{m+2}. \quad (29)$$

Due to the considerations expressed in the preceding sections, at increasing pressure the column temperature can be assumed constant only for certain diameter ranges, in each case (with the temperature increasing with increasing arc diameter).

Equation (29), or respectively, the constant in it, is hence valid only for those pressure ranges in which temperature changes can be neglected.

In order to allow a comparison between the analytically determined values, from equation (29) and the measurement results, the exponent  $m$  must be expressed numerically, with the aid of the family of curves (31). We accordingly obtain, for  $r = 1$  to 4,  $m = 1/2$ , which according to Figure 17, at 2A corresponds to a pressure range of 1 to 4 atm. Thus equation (29) becomes

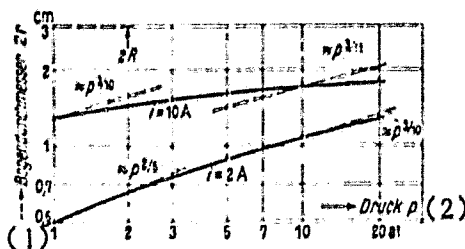
$$r = \text{const} \cdot p^{2/5}. \quad (30)$$

Similarly we furthermore obtain the values of  $m$  tabulated below (or for equation 29, respectively):

$r$ mm	Stromstarke A (1)	Gültiger Druckbereich at (2)	$m$
(1 ... 4	2	1 ... 4	1/2 $r \approx p^{2/5}$ )
5,5 ... 8	2	10 ... 20	4/3 $r \approx p^{3/10}$
5,5 ... 8	10	1 ... 5	4/3 $r \approx p^{3/10}$
8 ... 9	10	5 ... 20	5/3 $r \approx p^{5/11}$

KEY 1 Current intensity 2 Valid pressure range

Figure 34, below (page 51) compiles the experimentally (see Figure 17) and analytically [from equation (29)] determined pressure dependence of the arc diameter at 2 and 10 A. As can



KEY 1 Arc diameter  $2r$  2 Pressure  $p$

Figure 34 Comparison between measurement results from Figure 17 and the minimum theory. Arc diameter  $2r = f(p)$

be seen, the agreement is excellent, at  $2A$ .

For a larger current intensity of  $10A$ , the agreement between the theoretical and the experimental curves is not as good, for the reasons mentioned earlier.

After having concluded, from the considerations in sections V a and V b, with the aid of the measurement results for  $\mathfrak{E}$ ,  $i$  and  $r$ , that the column temperature in rotating arcs is independent of the carrier gas pressure, within certain limits, we shall now analytically determine the pressure dependence of the arc temperature, using the minimum principle.

β) Because of the temperature and pressure dependence of the thermal conductivity coefficient  $\lambda$ , we can approximate the energy equation (11) or (20), respectively, by

$$\mathfrak{E} \cdot i = \text{const} \cdot r^m \cdot T^{\alpha} \cdot p^{\beta}. \quad (31)$$

In conjunction with equation (26a):

$$i = \text{const} \cdot r^2 \cdot \mathfrak{E} \cdot n \cdot b$$

we obtain, eliminating  $r$ ,

/56

$$\mathfrak{E}^{m+1} \cdot i^{m-1} = \text{const} \cdot \frac{T^{\alpha} \cdot p^{\beta}}{n \cdot b}. \quad (32)$$

The number of electrons [see equation (3)] is  $n^- = x \cdot N$ , or approximately

$$n^- = \text{const.} \frac{T^{1/2}}{p},$$

because of the very small value of the degree of ionization  $x$ , in rotating arcs, where  $x$  is given by the ionization equation (2). The temperature and pressure dependence of the electron mobility is expressed by  $b^-$ :

$$b^- = \text{const.} \frac{T^{1/2}}{p}.$$

Therefore the product  $n^- \cdot b^-$  is:

$$n^- \cdot b^- = \text{const.} T^{1/2} \cdot p^{-1/2} \cdot 10^{-\frac{5040 + V_j}{2T}}. \quad (33)$$

According to the minimum theory, equation (32) must be differentiated with respect to  $T$

$$\left. \begin{aligned} \frac{d\psi}{dT} &= \text{const.} \frac{d}{dT} \left[ \frac{T^{1/2} \cdot p^{-1/2}}{T^{1/2} \cdot p^{-1/2} \cdot 10^{-\frac{5040 + V_j}{2T}}} \right] = 0 \\ \text{or} \quad \frac{d}{dT} \left( T^{1/2 - 3/4} \cdot p^{1/2 - 1/2} \cdot 10^{-\frac{5040 + V_j}{2T}} \right) &= 0 \end{aligned} \right\} \quad (34)$$

and solving for  $T$ :

$$T = \frac{5040 + \ln 10 + V_j}{2 \left( \frac{2s}{m} - 1/2 \right)}. \quad (35)$$

While in equation (35) the pressure itself does not appear, this does not of itself mean pressure independence, for the temperature: the values of the exponents  $m$  and  $s$  and the resulting value of the ionization potential  $V_j$  do change with pressure. The pressure dependence of the resulting ionization potential for nitrogen is very low, however, ( $V_j \approx p^{-1/20}$ ) and can hence be disregarded.

The exponent  $s$ , which indicates the severity of the temperature dependence of the thermal conductivity  $\lambda$ , increases from

approximately 4 to 7, for the the temperatures between 5000°K and 6500°K that occur in rotating arcs in nitrogen. Since in this case the pressure was particularly taken into consideration, it no longer appears here.

The exponent  $m$  undergoes the greatest changes, as a function of pressure, for instance from 1/2 at 1 atm and 2 A, to 3/4 at 20 atm, as already established.

It follows that the temperature of the rotating arc depends almost exclusively on  $m$ , i.e., that at constant column radius the temperature is independent of the pressure, and that as the radius increases, so does the arc column's temperature.

But then the statement of the minimum theory is in excellent agreement with experiment, also with respect to the pressure dependence of the arc temperature, because even though the arc temperature was not measured in these experiments, the considerations expressed in sections Va and Vb on the basis of measurements of the longitudinal field intensity, the current density and the column diameter have led to the just described result on pressure dependence of the temperature, without applying the principle of the lowest burning tension.

We shall not attempt a theoretical examination of the conditions /57 of the rotating arc in carbon dioxide, because of the currently only deficient knowledge regarding the considerably involved elementary processes and hence, because of the impossibility of calculating the pressure dependence, for instance, of the number of electrons, or of the additional thermal conductivity, within the context of this study.

A more precise examination of the minimum principle on the basis of the measurement results here accumulated, by a different, much more general method, will be performed in M. Steenbeck's following article. There is also excellent agreement between calculation and measurement.

## VI CONCLUSION

The investigations here described were performed at the High Voltage Institute "Neubabelsberg" of the Berlin Institute of Technology.

I am deeply indebted to the Institute's Director, professor A. Matthias, for making this study possible and for his interest. I would also like to thank the former scientific assistants of this Institute, graduate engineers Czemper and Mochow, for their help in the design of the test equipment.

## REFERENCES

/58

- 1 Duncan, L., Rowland, A. J. and Todd, R. J., Der elektrische Lichtbogen under Druck [The electric arc under pressure], ETZ 14, 603 (1893)
- 2 Lummer, O., Verfluessigung der Kohle und Herstellung der Sonnentemperatur [Coal liquefaction and the production of solar temperatures]. Brunswick (1914)
- 3 Luckey, G. P., The tungsten arc under pressure, Phys. Rev. 9(2), 129 (1917)
- 4 Mathiesen, W., Untersuchungen ueber den elektrischen Lichtbogen [Investigations on the electric arc], Leipzig (1921)
- 5 Schoenherr, P., ETZ 30, 365 (1909)
- 6 Traub, E., Ueber rotierende Stroemungen in Rohren und ihre Anwendung zur Stabilisierung von elektrischen Flammenbogen [Rotating currents in tubes and their application to the stabilization of luminous electric arcs], Ann. Phys. 18(5), 169 (1933)
- 7 Grotian, W., Der Gleichstrom-Lichtbogen grosser Bogenlaenge [The direct current arc of great arc length], Ann. Phys. 47(5), 141 (1915)

- 8 von Engel, A., Elektrische Messungen an langen Gleichstromlichtbogen in Luft [Electric measurements on long direct current arcs in air], Z.techn.Phys. 10, 505 (1929)
- 9 von Engel, A. and Steenbeck, M., "Elektrische Gasentladungen I und II [Electric discharges in gases, I and II], Berlin (1932 and 1934)
- 10 von Engel, A. and Steenbeck, M., Ueber die Temperatur in der Gassaeule eines Lichtbogens [The temperature of the gas column in an arc], Wiss.Veroeff. Siemens X(2), 155 (1931)
- 11 Ramsauer, C., Ueber die Temperatur des elektrischen Lichtbogens [The temperature of the electric arc], Elektrotechn. u.Masch.Bau 51, 189 (1933)
- 12 Kirschstein, B. and Koppelmann, F., Photographische Aufnahmen elektrischer Lichtboegen grosser Stromstaerke [Photographs of high current intensity electric arcs], Wiss. Veroeff. Siemens XIII (3), 52 (1934)
- 13 Holm, R. and Lotz. A., Messungen der Gesamtstrahlung der Saeule eines Wechselstrombogens in Luft [Measurements of the total radiation from the column of an alternate current arc in air], Wiss.Veroeff. Siemens XIII (2), 87 (1934)
- 14 Mayr, O., Hochleistungsschalter ohne Oel [High-capacity circuit breaker without oil], ETZ 53, 75 (1932)
- 15 Biermanns, J., Ueber den Unterbrechungsvorgang im Hochleistungsschalter [The interruption process in the high-capacity circuit breaker], ETZ 53, 641 (1932)
- 16 Steenbeck, M., Energetic der Gasentladungen [Energetics of gas discharges], Phys.Z. 33, 809 (1932)
- 17 Elenbaas, W., Kesselring, F. and Koppelmann, F., Zur Frage der Berechtigung des Minimumprinzip in der Theorie der Bogentladung [The question of the applicability of the minimum principle to the theory of arc discharges], ETZ 57 (Correspondence), 1497 (1936)

- 18 Kesselring, F., Untersuchungen an elektrischen Lichtboegen [Studies of electric arcs], ETZ 55, 92 (1934)
- 19 Holm, R., Kirschstein, B. and Koppelman, F., Ueberblick ueber die Physik des Starkstromlichtbogens mit besonderer Beruecksichtigung der Loeschung in Hochleistungs-Wechselstromschaltern [Review of the physics of power current arcs, with special consideration for their extinction in high-capacity alternate current switches], Wiss. Veroeff. Siemens XIII (2), 63 (1934)
- 20 Kirschstein, B. and Koppelman, F., Beitrag zur Minimum-theorie der Lichtbogensaeule. Vergleich zwischen Theorie und Erfahrung [Contribution to the minimum-theory of the electric arc column. Comparison between theory and experience], Wiss. Veroeff. Siemens XVI (3), 56 (1937)
- 21 Schottky, W., Wandstroeme und Theorie der positiven Saeule, [Wall currents and the theory of the positive column], Phys. Z. 25, 342 (1924)
- 22 Compton, K. T. and Langmuir, F., Rev.Mod.Phys. 2, 218 (1930)
- 23 Saha. M. N., Versuch einer Theorie der physikalischen Erscheinungen bei hohen Temperaturen [Attempt at a theory of the physical phenomena at high temperatures], Z.Phys. 6, 40 (1921)
- 24 Ter Horst, Brinkmann, H. and Ornstein, L. G., Der zeitliche Verlauf der Temperatur in Bogenentladungen mit Wechselstrom [The temporal course of the temperature in alternate current arc discharges], Physica II (7), 652 (1935)
- 25 Chwolson, O. D., "Lehrbuch der Physik" [Textbook of Physics] III (1905)
- 26 Ornstein, L. S., Brinkmann, H. and Bennes, A., Pruefung der Comptonschen Bogentheorie durch Messungen der Bogentemperatur als Funktion des Druckes [Test of Compton's arc theory by arc temperature measurements as a function of pressure], Z.Phys. 77, 72 (1932)